



23 \*Correspondence: Mónica V. Cunha, Centre for Ecology, Evolution and Environmental  
24 Changes (cE3c), Faculdade de Ciências, Universidade de Lisboa, Campo Grande, 1749-016  
25 Lisboa, Portugal. Email: [mscunha@ciencias.ulisboa.pt](mailto:mscunha@ciencias.ulisboa.pt)

26 **ABSTRACT**

27 As the COVID-19 pandemic reached its peak, many countries implemented genomic  
28 surveillance systems to track the evolution and transmission of SARS-CoV-2. Transition from  
29 the pandemic to the endemic phase prioritized alternative testing strategies to maintain  
30 effective epidemic surveillance at the population level, with less intensive sequencing efforts.  
31 One such promising approach was Wastewater-Based Surveillance (WBS), which offers  
32 non-invasive, cost-effective means for analysing virus trends at the sewershed level. From  
33 2020 onwards, wastewater has been recognized as an instrumental source of information for  
34 public health, with national and international authorities exploring options to implement  
35 national wastewater surveillance systems and increasingly relying on WBS as early warning  
36 of potential pathogen outbreaks. In Portugal, several pioneer projects joined the academia,  
37 water utilities and Public Administration around WBS.

38 To validate WBS as an effective genomic surveillance strategy, it is crucial to collect long  
39 term performance data. In this work, we present one year of systematic SARS-CoV-2  
40 wastewater surveillance in Portugal, representing 35% of the mainland population. We  
41 employed two complementary methods for lineage determination - allelic discrimination by  
42 RT-PCR and S gene sequencing. This combination allowed us to monitor variant evolution in  
43 near-real-time and identify low-frequency mutations.

44 Over the course of this year-long study, spanning from May 2022 to April 2023, we  
45 successfully tracked the dominant Omicron sub-lineages, their progression and evolution,  
46 which aligned with concurrent clinical surveillance data. Our results underscore the  
47 effectiveness of WBS as a tracking system for virus variants, with the ability to unveil  
48 mutations undetected via massive sequencing of clinical samples from Portugal,  
49 demonstrating the ability of WBS to uncover new mutations and detect rare genetic variants.

50 Our findings emphasize that knowledge of the genetic diversity of SARS-CoV-2 at the  
51 population level can be extended far beyond via the combination of routine clinical genomic  
52 surveillance with wastewater sequencing and genotyping.

53

54 **KEYWORDS**

55 SARS-CoV-2; Spike gene sequencing; Wastewater-Based Surveillance; Wastewater  
56 sequencing; Genomic variants.

57

58 **INTRODUCTION**

59 During the coronavirus disease 2019 (COVID-19) pandemic, detection of severe acute  
60 respiratory syndrome coronavirus 2 (SARS-CoV-2) in faeces accelerated the introduction of  
61 wastewater surveillance in a variety of settings, including cities, airports, hospitals, and  
62 university campuses (Agrawal et al., 2021; Medema et al., 2020; Nkambule et al., 2023). At  
63 the population level, wastewater-based surveillance (WBS) has been implemented solely as  
64 a complementary method to clinical surveillance (Peccia et al., 2020). However, WBS  
65 enabled correlating the real-time information of SARS-CoV-2 viral loads in sewage with the  
66 increase of positive cases and hospitalizations (Galani et al., 2022; Perez-Zabaleta et al.,  
67 2023), in addition to the identification of outbreak hotspots within a given region at the  
68 sewershed level (Fontenele et al., 2021; Medema et al., 2020; Monteiro et al., 2022).  
69 Moreover, WBS has also enabled detection of novel SARS-CoV-2 mutations in urban  
70 wastewater, which had not been detected by standard clinical surveillance (Karthikeyan et  
71 al., 2022; Smyth et al., 2022). WBS has thus become a public health instrument helping to  
72 track SARS-CoV-2 spread.

73 Given the potential contribution of both symptomatic and asymptomatic shedder individuals  
74 to SARS-CoV-2 viral load in sewage (Elsamadony et al., 2021; Foladori et al., 2020; Wu et  
75 al., 2020), wastewater surveillance presents a less biased and resource-effective approach  
76 for obtaining an overview of the viral diversity circulating in a community, in contrast to the  
77 currently dominant approach of clinical genomic surveillance. Therefore, in recognition of the  
78 immense potential of WBS, the European Commission recommended to Member States the

79 implementation of regular SARS-CoV-2 monitoring through molecular analyses and  
80 sequencing of wastewater (*Commission Recommendation (EU) 2021/472*, 2021). Hence, a  
81 considerable number of studies with diverse aims, from establishing methodologies to finding  
82 new mutations, have reported results from WBS of European sub-populations (Agrawal et  
83 al., 2021; Amman et al., 2022; Galani et al., 2022; Izquierdo-Lara et al., 2021, 2023;  
84 Katharina et al., 2022; La Rosa et al., 2023; Medema et al., 2020; Monteiro et al., 2022;  
85 Pérez-Cataluña et al., 2022; Perez-Zabaleta et al., 2023). However, it is important to note  
86 that such studies are not limited to Europe; similar investigations have been conducted in  
87 American (Crits-Christoph et al., 2021; Fontenele et al., 2021; Gregory et al., 2022;  
88 Karthikeyan et al., 2022; Nemudryi et al., 2020; Peccia et al., 2020; Sapoval et al., 2023;  
89 Silva et al., 2022; Smyth et al., 2022; Swift et al., 2022) and Asian (Bar-Or et al., 2021) sub-  
90 populations as well. The data collected are of significant importance for comprehending  
91 methodological challenges and uncertainty sources, comparing the performance of WBS  
92 versus clinical surveillance, and extracting additional valuable information from WBS data.

93 The COVID-19 pandemic has been characterized by the sequential emergence of various  
94 variants of interest and variants of concern (VOC), with the most recent being Omicron  
95 (pangolin lineage B.1.1.529), initially identified in November 2021 (Rambaut et al., 2020;  
96 WHO, 2023). These VOCs are characterized by constellations of mutations that, to various  
97 degrees, appear to impact on virus transmissibility, clinical outcome, evasion from vaccine-  
98 derived adaptive immune responses, and effectiveness of diagnostic tests (Khateeb et al.,  
99 2021; Kuzmina et al., 2022; Tao et al., 2021). To date, wastewater analysis has routinely  
100 employed two approaches: (i) reverse transcription quantitative PCR (RT-qPCR) or reverse  
101 transcription-droplet digital PCR (RT-ddPCR) for SARS-CoV-2 detection and quantification;  
102 and (ii) high-throughput sequencing for monitorization of SARS-CoV-2 mutations and  
103 variants (Bar-Or et al., 2021; Crits-Christoph et al., 2021; Nemudryi et al., 2020). Although  
104 PCR-based wastewater surveillance enables the quick and highly sensitive detection and  
105 quantification of virus load in sewage, with the possibility to target specific viral mutations, it  
106 can provide limited information on which lineages and/or variants are circulating, because the

107 number of diagnosing mutations has greatly decreased with the increase of viral genetic  
108 diversity concurrent with the expansion of the Omicron VOC. Tracking SARS-CoV-2 genetic  
109 diversity thus became essential to detect precociously the emergence of novel SARS-CoV-2  
110 variants with potentially higher transmissibility and/or immune evasion properties, demanding  
111 rapid, cost-efficient, and accessible methods.

112 In this work, we aimed to monitor SARS-CoV-2 variant evolution in near-real-time and  
113 identify both major and low-frequency mutations. For that purpose, we present one year of  
114 systematic SARS-CoV-2 wastewater surveillance in Portugal, during the implementation of  
115 the European Commission (EC) Recommendation no. 2021/472, representing about 35% of  
116 the mainland population. We performed a combined approach, using a series of allele-  
117 specific RT-PCR assays targeting a panel of six Omicron associated mutations chosen to  
118 differentiate the most prevalent circulating lineages, and targeted Illumina sequencing of the  
119 Spike (S) gene of wastewater samples recovered in Portugal between May 2022 and April  
120 2023.

121

## 122 **MATERIALS AND METHODS**

### 123 **Study design, wastewater sampling and SARS-CoV-2 detection**

124 The national surveillance system set up during the implementation of the EC  
125 Recommendation no. 2021/472 in Portugal aimed to cover a significant part of the  
126 Portuguese population. Given the dimension of the agglomerations on the national territory,  
127 the wastewater treatment plants (WWTPs) monitored for SARS-CoV-2 were selected based  
128 on facilities serving more than 100000 equivalent population and by excluding WWTPs with a  
129 strong industrial component. Monitorization focused on 14 WWTPs from the largest cities of  
130 the country, reflecting 34.2% of the mainland population. One litre of 24-hour composite raw  
131 wastewater samples was collected twice a week from 14 WWTPs located in the North  
132 (*number of WWTPs, n=4*), Center (*n=2*), Lisbon and Tagus Valley (LTV) (*n=4*), and Algarve  
133 (*n=4*) regions (Figure S1), with a population equivalent ranging from 113200 to 920000.  
134 Wastewater collection took place between May 2022 and April 2023 resulting in a total of  
135 1339 samples.

136 Wastewater processing, RNA extraction, detection, and quantification were performed as  
137 previously described by Monteiro *et al.* 2022 (Monteiro et al., 2022). The SARS-CoV-2 viral  
138 load in each sample was estimated via viral RNA detection through RT-qPCR using the  
139 Charité assays: the E\_Sarbeco assay targeting the envelope protein gene, the RdRp assay  
140 targeting the RNA-dependent RNA polymerase gene, and the N\_Sarbeco assay targeting  
141 the nucleoprotein (Corman et al., 2020). For these, the one-step RT-qPCR assays AgPath-  
142 ID™ One-Step RT-PCR (Thermo Fisher Scientific, USA) were used as described before  
143 (Monteiro et al., 2022).

144

### 145 **Allelic discrimination analysis to detect Omicron associated mutations in wastewater** 146 **samples**

147 A set of six commercially available probe-based genotyping RT-PCR assays was used for  
148 the identification of mutations associated to specific Omicron sub-lineages. The panel of  
149 allele discrimination assays was continuously updated throughout the sampling period to

150 accommodate variation within circulating Omicron sub-lineages, as assessed by clinical  
151 epidemiologic surveillance (Figure S2). These genotyping assays targeted specific amino  
152 acid changes, namely G339D, L452R, Q493R and T475K at S gene, D3N at M gene, and  
153 L11F at ORF7b (Table S1).

154 Genotyping assays were performed using the TaqMan SARS-CoV-2 Mutation Panel  
155 (Thermo Fisher Scientific, USA) following the manufacturer's instructions. Each reaction  
156 consisted of 5 µL of wastewater RNA, mixed with 4X TaqPath™ 1-Step RT-qPCR Master  
157 Mix CG (Thermo Fisher Scientific, USA) and 40X TaqMan probes (Thermo Fisher Scientific,  
158 USA), in a final volume of 20 µL. Each assay included sequence-specific forward and  
159 reverse primers to amplify the target region and two TaqMan minor groove binder (MGB)  
160 probes with non-fluorescent quenchers (NFQ) to detect the PCR-amplification fragments:  
161 one FAM dye-labelled probe binds the mutated gene, and one VIC dye-labelled probe binds  
162 the wild-type SARS-CoV-2 gene.

163 PCR cycling was performed on a StepOne™ Real-Time PCR System (Applied  
164 Biosystems™), under the following conditions: reverse transcription at 45°C for 15 minutes,  
165 Taq polymerase activation at 95°C for 2 minutes, followed by 45 cycles of denaturation at  
166 95°C for 15 seconds, and annealing at 58°C for 45 seconds, with a final post-read for 30  
167 seconds at 60°C. All RT-PCR experiments included a no-template control (NTC) (*i.e.*,  
168 DNase/RNase free water), and a wild-type AcroMetrix Coronavirus 2019 (COVID-19) RNA  
169 control (RUO) (Thermo Fisher Scientific).

170 Allelic discrimination results were then visualized on a scatter plot, contrasting reporter dye  
171 fluorescence (*i.e.*, mutated allele versus wild type allele), and analyzed using QuantStudio  
172 Design and Analysis Software version 2.5, via the genotyping analysis module with real-time  
173 data.

174

### 175 **S gene sequencing and reference-based analyses**

176 From the complete set of samples, 332 were selected for S gene sequencing. These  
177 corresponded to two samples per month and per WWTP, as defined in the EC



178 Recommendation. Whenever possible, the samples selected for sequencing were those that  
179 exhibited RT-qPCR amplification of at least two SARS-CoV-2 genes (E, N, or RdRp), with  
180 threshold cycle (Ct) values below 36, which were found to yield more genome coverage.  
181 Samples with higher Ct values were preferentially avoided to ensure best quality sequencing  
182 results and facilitate accurate SARS-CoV-2 variant/lineage assignment.

183 The RNA from the wastewater samples was purified with RNeasy MinElute Cleanup kit  
184 (Qiagen), following the manufacturer's instructions, to eliminate impurities and inhibitors that  
185 could potentially interfere with the subsequent sequencing process. Total RNA was then  
186 quantified using the Qubit RNA HS Assay kit (Thermo Fisher Scientific, USA), following the  
187 manufacturer's instructions. Samples with RNA concentrations above 20 ng/μl were selected  
188 for SARS-CoV-2 sequencing.

189 The SARS-CoV-2 target amplicon libraries were constructed using ARTIC SARS-CoV-2 RNA  
190 library (Eurofins, Konstanz, Germany), which was especially designed to amplify the S gene.  
191 Sequencing occurred using the Illumina NovaSeq 6000, according to the manufacturer's  
192 specifications, with the paired-end module (2x150 bp) attachment. Eurofins sequencing  
193 strategy was optimized for the S gene sequencing in wastewater samples, with the  
194 application of 49 primers, including 22 primer pairs with 5 alternative primers to account for  
195 variability in the primer binding region. The 22 amplicons ranged in size from 200 to 250  
196 base pairs, and collectively cover the entire S-gene sequence, spanning 3822 base pairs.

197 Read processing, reference-based alignment and variant analysis were performed using  
198 bioinformatics tools available in the Galaxy EU server (Afgan et al., 2018). Quality control  
199 reports were generated with FastQC (Galaxy version 0.11.9) using default parameters. Raw  
200 reads were cleaned up from adaptors (-ILLUMINACLIP) and low quality nucleotides (-  
201 SLIDINGWINDOW:4:30) using Trimmomatic (Galaxy version 0.38) (Bolger et al., 2014).  
202 Quality trimmed reads were aligned to the SARS-CoV-2 reference genome (NCBI accession  
203 number NC\_045512.2) using the Burrows-Wheeler Aligner (Galaxy version 0.7.17) (Li, 2013)  
204 with default parameters; and reads with less than 35 bp were removed, using BAM filter  
205 (Galaxy version 0.5.9) in order to eliminate primers and short uninformative reads. Variant

206 calling was performed using iVar pipeline (Galaxy version 1.4.2) (Grubaugh et al., 2019), with  
207 the minimum quality score threshold to count a base being set to 20, and the minimum  
208 frequency threshold to 0.03. The minimum number of reads to consider major variants  
209 (polymorphism with a frequency above 0.5) was set to 10, while for minor variants  
210 (polymorphism with a frequency between 0.03 and 0.49) the number of supporting reads was  
211 set to 20.

212 The nucleotide polymorphisms were evaluated considering their effect on their protein  
213 product by SnpEff (Galaxy version 4.5covid) (Cingolani et al., 2012). Finally, the quality  
214 metrics of the assemblies were obtained with Qualimap BAMQC (Galaxy version 2.2.2)  
215 (Okonechnikov et al., 2016).

216 Information concerning the worldwide occurrence of specific SARS-CoV-2 genetic  
217 polymorphisms and frequency was obtained from outbreak.info (Gangavarapu et al., 2023).

218

### 219 **SARS-CoV-2 lineage assignment**

220 To perform SARS-CoV-2 lineage assignment, Freyja pipeline (Karthikeyan et al., 2022),  
221 currently available at <https://github.com/andersen-lab/Freyja>, was used. Freyja is a  
222 bioinformatics pipeline designed to estimate the relative abundance of SARS-CoV-2 lineages  
223 in a mixed sample. To assign a lineage to each sample, Freyja stores the single nucleotide  
224 polymorphism (SNP) frequencies for each of the lineage-defining mutations and recovers  
225 relative lineage abundance by solving a depth-weighted least absolute deviation regression.  
226 Note that greater sequencing depth estimate mutation frequencies more accurately, which  
227 results in more precise lineage assignments. Freyja assigns SARS-CoV-2 lineages based on  
228 the outbreak.info curated lineage metadata file that summarizes lineages by World Health  
229 Organization (WHO) designation.

230

### 231 **Data analysis**

232 SARS-CoV-2 lineage assignment and mutation data derived from clinical surveillance were  
233 obtained from GISAID (<https://www.gisaid.org/>, accessed on the 20<sup>th</sup> of June 2023) (Elbe and

234 Buckland-Merrett, 2017; Shu and McCauley, 2017). Clinical samples from Portugal, with  
235 collection dates ranging between the 19<sup>th</sup> of April 2022 and the 12<sup>th</sup> of May 2023,  
236 comprehending the wastewater sample collection period plus two weeks before and  
237 afterward, were selected. This dataset was further filtered to samples isolated in the Health  
238 Regions covered by the WWTPs under monitoring in this study (*i.e.*, North, Center, Lisbon  
239 and Tagus Valley, and the Algarve) (Figure S1).

240 Data analysis and visualization was performed with custom Python 3.9.10 (Van Rossum and  
241 Drake, 2009) and R version 4.1.1 (R Core Team, 2021) scripts. Python modules pandas  
242 version 1.4.1 (McKinney, 2010) isoweek version 1.3.3, outbreak\_data version 1.0.1, and  
243 numpy version 1.22.3 (Harris et al., 2020) were used for data manipulation. R packages dplyr  
244 version 1.1.2 (Wickham et al., 2023a), ggplot2 version 3.4.2 (Wickham, 2016), gridExtra  
245 version 2.3 (Aguie and Antonov, 2017) gtable version 0.3.3 (Wickham et al., 2023c), readr  
246 version 2.1.4 (Wickham et al., 2023b) BiocManager version 1.30.20 (Morgan and Ramos,  
247 2023) drawProteins version 1.14.0 (Brennan, 2018), ggforce version 0.4.1 (Pedersen, 2022)  
248 and cowplot version 1.1.1 (Wilke, 2020) were used to create the visualizations in RStudio  
249 version 1.4.1717 (RStudio Team, 2021). Spike protein annotations were obtained from  
250 UniProt (accession number: P0DTC2; (The UniProt Consortium, 2023)); mutation occurrence  
251 per country was retrieved from outbreak.info (Gangavarapu et al., 2023) using the R package  
252 outbreakinfo version 0.2.0 (Alkuzweny et al., 2023); the number of sequences made  
253 available per country was retrieved from GISAID (Elbe and Buckland-Merrett, 2017; Shu and  
254 McCauley, 2017); and the Simpson evenness index was calculated using R package abdiv  
255 version 0.2.0 (Bittinger, 2020).

256 **RESULTS**

257 **The adaptive combination of RT-PCR allelic discrimination assays successfully**  
258 **captures the co-occurrence and progression of the main Omicron sub-lineages**

259 All the 1339 wastewater samples under focus in this study were tested for the presence of  
260 specific mutations associated to one or several Omicron sub-lineages. Given the fast  
261 evolution of Omicron sub-lineages, the panel of applied genotyping assays was regularly  
262 updated (Figure S2) throughout the sampling period to discriminate new sub-lineages. This  
263 meant adding new assays targeting diagnostic mutations of new sub-lineages and halting  
264 assays that no longer had discrimination power over the sub-lineages circulating in that  
265 period. These decisions were informed both by the results that were being obtained weekly,  
266 as well as by the clinical surveillance data made publicly available by the Directorate-General  
267 of Health (DGS) and the National Institute of Health Doutor Ricardo Jorge (INSA, 2021).

268 At sampling starting point, four genotyping assays were applied. The genotyping assay that  
269 detected a signature mutation of the Omicron VOC (*i.e.*, S:G339D) was selected to assess  
270 the circulation of older VOCs that possess the wild-type allele. Note that at the beginning of  
271 the sampling period, Omicron was already the dominant VOC. With the exception of ISO  
272 week 24, the mutant allele was exclusively detected until September 2022 (ISO week 38),  
273 from which point both alleles were regularly identified (Figure S3). Clinical surveillance data  
274 for all analyzed regions (Figure 1A) showed that, at that time point, the resurgence of older  
275 VOCs was not being observed, but instead detection of the wild type allele corresponded to  
276 the emergence of Omicron sub-lineages without this mutation, among them the recombinant  
277 sub-lineages of CH and XBB (named hereafter CH.X and XBB.X). Given that this mutation  
278 was no longer a signature mutation for the Omicron VOC, we suspended the application of  
279 this assay in the beginning of November 2022 (week 45).

280 Another assay applied at the beginning of our sampling period was able to identify the  
281 signature mutation of the Omicron BA.1 lineage and its daughter lineages (BA.1.X; S:T475K;  
282 Figure S2). However, we have only applied this assay during the first two weeks of the  
283 sampling period (weeks 18 and 19) given that the mutant allele was never amplified in any

284 sample (Figure S3). This observation supported the hypothesis that BA.1.X sub-lineages  
285 were no longer circulating in the analyzed communities, which agreed with the clinical  
286 epidemiological data (Figure 1A) and led to the early exclusion of this assay from the panel.  
287 Between May 2022 (week 18) and November 2022 (week 48) the genotyping assay that  
288 identifies the S:Q493R mutation present in BA.1.X, BA.2.X and BA.3.X Omicron sub-lineages  
289 was applied (Figure S2). Knowing that BA.3.X had only been detected twice in Portugal  
290 through genome sequencing and before the start of our sampling period, and also being  
291 aware that BA.1.X was being reported from week 16 in percentages below 1%, the  
292 identification of the mutant allele S:Q493R was presumed indicative of BA.2.X circulation.  
293 Between ISO weeks 18 and 29, the clinical data shows the substitution of BA.2.X by BA.5.X  
294 (Figure 1A). BA.2.X sub-lineages were dominant in the clinical data until week 19,  
295 representing over 50% of the available sequences. In wastewater samples, the mutant allele  
296 of S:Q493R was detected in over 50% of samples for five weeks longer (*i.e.*, until week 24)  
297 but also with a decreasing tendency (Figure S3). Interpretation of results for samples with  
298 amplification of the mutant allele only, without amplification of the wild type allele, was  
299 translated as the presumable presence of 100% BA.2.X sub-lineages in the wastewater  
300 samples. Detection of this mutant allele stopped at week 20, after which amplification of both  
301 alleles was obtained, suggesting the coexistence of both BA.2.X and BA.5.X sub-lineages in  
302 the same sample. Similar results were observed at regional level, with the mutant allele of  
303 S:Q493R amplified in over 50% of samples until week 23 in Algarve, and until week 24 in  
304 North, Center and, Lisbon and Tagus Valley (LTV) regions (Figure S4). The identification of  
305 samples only with the amplification of the mutant allele stopped at week 19 in the North,  
306 Center and LTV regions, and at week 20 at Algarve. Despite the similarities, the increase in  
307 detection of the wild type allele, and consequently the decrease of BA.2.X detection, was  
308 faster in the LTV region, followed by Algarve, North and Center regions (Figure S4).  
309 The mutation S:L452R is present in BA.4.X, BA.5.X and BA.2.35, and was also applied from  
310 the beginning of our sampling period and until week 29. Since the percentage of BA.4.X  
311 sequences isolated until week 29 was residual, the presence of the mutant allele was taken

312 as an indication of the presence of BA.5.X or BA.2.35 sub-lineages. The combination of  
313 results from genotyping assays S:Q493R and S:L452R resolved the ambiguity of the assay  
314 for mutation S:Q493R in lineage assignment and allowed detecting the presence of BA.2.35  
315 sub-lineage. Based on this, sub-lineage BA.2.35 was presumably present in Portugal at least  
316 until week 24.

317 At week 29, two new assays were added (Figure S2): the genotyping assay ORF7b:L11F,  
318 which identifies a signature mutation of BA.4.X sub-lineage, that was applied until the end of  
319 2022 (week 52); and the genotyping assay M:D3N, which identifies the signature mutation of  
320 BA.5.X, that was applied until April 2023 (week 17).

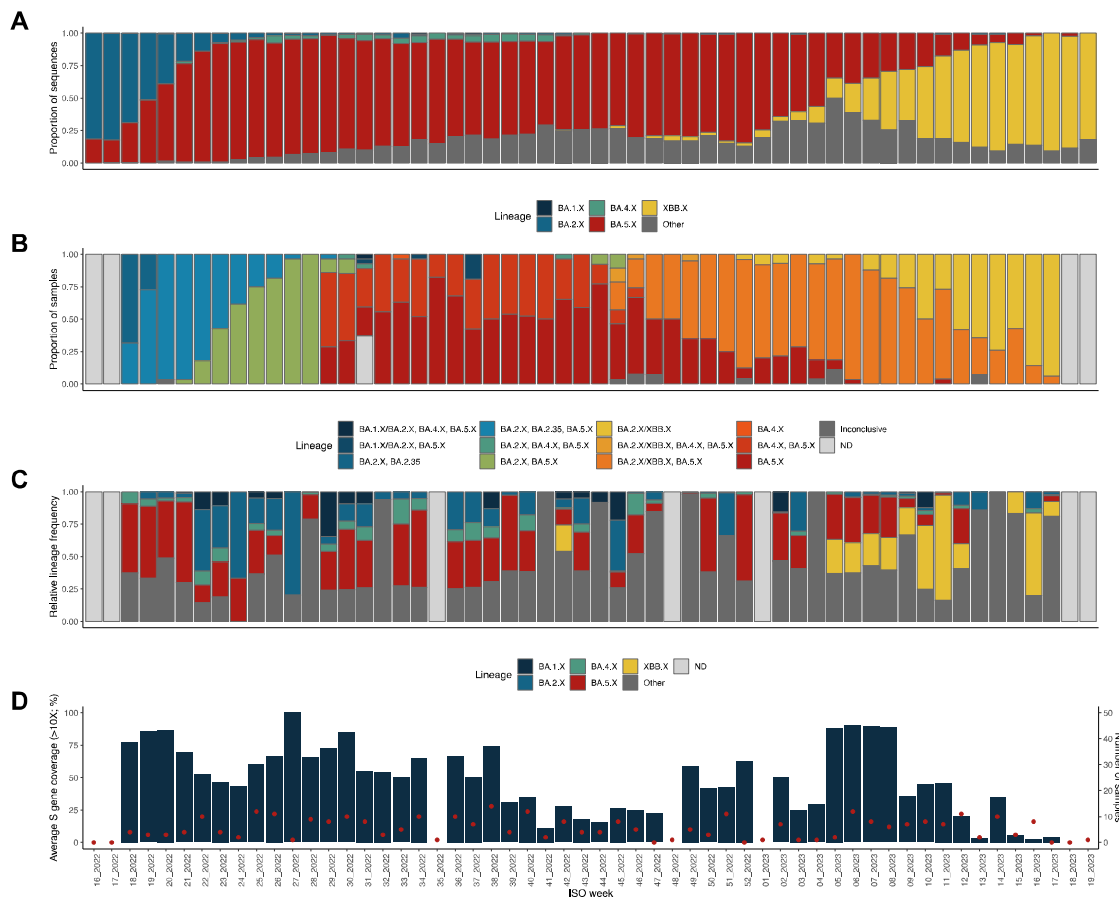
321 Concerning BA.4.X sub-lineage, none of the analyzed samples revealed the unique  
322 amplification of the mutant allele, indicating that the presence of BA.4.X was concomitant at  
323 all times with BA.5.X. From week 29 until week 34, the signature mutation of BA.4.X was  
324 identified in most samples. At the national scale, the last reported detection of this lineage on  
325 clinically derived sequences is dated from week 48, while in wastewater samples the mutant  
326 allele was amplified until week 49. Considering the regional stratification, the identification of  
327 BA.4.X in wastewater continued to be reported later in time when comparing with clinical  
328 data (Figures 1, S4 and S5), except for the Center region. Specifically, at the Algarve, BA.4.X  
329 was last identified in wastewater at week 46, while in clinical data was at week 40; at LTV it  
330 was last reported in wastewater at week 49, while at clinical data was at week 43; at North, it  
331 was detected up to week 45 in wastewater and at week 43 in clinical data (Figure S5). The  
332 center region clinical data reported BA.4.X until week 48, while in wastewater it was detected  
333 up until week 46. Since the mutant allele was not detected at wastewater samples in the last  
334 three weeks of 2022, we suspended the implementation of the genotyping assay  
335 ORF7b:L11F in the end of 2022.

336 Regarding BA.5.X, the mutant allele (*i.e.*, M:D3N) was identified in all samples recovered  
337 between week 29 of 2022 and week 17 of 2023 (Figure S3), attesting the uninterrupted  
338 circulation of BA.5.X. This is in agreement with the clinical data that shows BA.5.X with an  
339 increased and dominant tendency until the end of 2022, when XBB.X started increasing their

340 frequency (Figure 1). At the regional level, the scenario is similar, with the mutant allele  
341 amplified in over 50% of samples until week 13 of 2023 at North region, until week 12 at  
342 national level and at LTV region, until week 10 at Center region, and until week 9 at Algarve  
343 region (Figure S4). This shows that the substitution of BA.5.X by XBB.X was faster at  
344 Algarve region, followed by Center, then LTV and later in the North region.

345 Figure 1B presents a comprehensive summary of the wastewater data, enabling the easy  
346 comparison between the results from RT-PCR genotyping assays and the clinical data  
347 presented in Figure 1A. The samples are grouped by week, and the categories represent all  
348 the sub-lineages found in each sample. Note that, for 21 samples, the allele discrimination  
349 analysis was inconclusive due to lack of amplification, which might be due to the complex  
350 nature of wastewater samples that can contain PCR inhibitors and other contaminants.  
351 Another possible reason for the lack of amplification in these samples concerns the  
352 sensitivity of the assays. In fact, the manufacturer recommends the assays to be applied to  
353 samples whose Ct was inferior to 30 in the RT-qPCR for SARS-CoV-2 identification, which  
354 was not the case for any of these samples.

355



356

357 **Figure 1: Lineage frequency evolution.** **A.** Lineage assignment of sequences derived from clinical  
 358 genomic surveillance. The samples were collected in Portugal (in North, Center, Lisbon and Tagus  
 359 Valley, and Algarve Health Regions) between ISO week 16 of year 2022 and ISO week 19 of year  
 360 2023. Lineages were grouped with all descendant lineages of the five major circulating sub-lineages  
 361 (BA.1, BA.2, BA.4, BA.5 and XBB) grouped into a single category. The remaining (minor) lineages  
 362 were grouped into a single category (Other). **B.** Lineage assignments in WWTP samples based on  
 363 real-time PCR diagnostic data (allelic discrimination assays). Based on the tested alleles, the samples  
 364 were grouped into 14 categories. Most of the categories group samples in which multiple major  
 365 circulating lineages were detected. The forward slash indicates that the test cannot distinguish  
 366 between the two lineages. In a small number of samples, amplification was not obtained in all  
 367 necessary real-time PCR assays and hence they were grouped in the category “Inconclusive”.  
 368 Samples not tested were grouped in the Not Determined (ND) category. **C.** Lineage assignments in  
 369 WWTP samples based on sequencing data. The data was grouped in the same categories as those in  
 370 panel A for convenience of comparison. **D.** Average horizontal S gene sequencing coverage and  
 371 number of sequenced samples per week (referring to the data presented in panel C). Vertical blue bars  
 372 represent the average horizontal coverage of that week’s samples, and red dots represent the  
 373 number of sequenced samples on that week. Note that ISO weeks 16 and 17 of 2022 and ISO weeks  
 374 18 and 19 of 2023 were out of our wastewater sampling period. On ISO week 35 of 2022, there was  
 375 no sampling at all, and on ISO weeks 48 of 2022 and 01 of 2023, no samples were sequenced due to  
 376 the low quality of the samples’ RNA.

377

378



## 379 **S gene sequencing exhibits high sensitivity to sample quality variations**

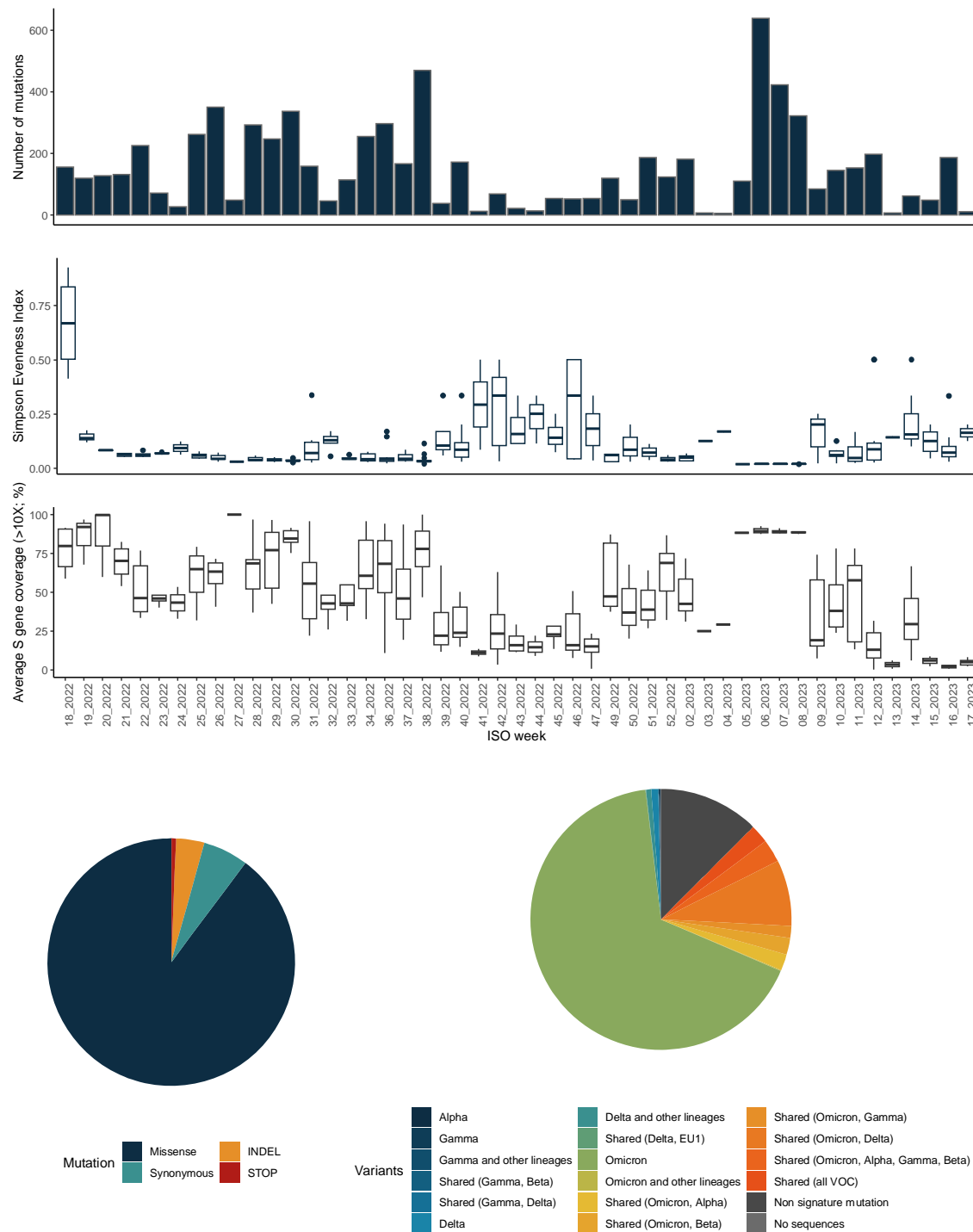
380 From the initial pool of 1339 samples, 332 were selected for S gene sequencing based on  
381 specific criteria: RNA concentration above 20 ng/ $\mu$ l, Ct values of the RT-qPCR for SARS-  
382 CoV-2 detection below 36, and the inclusion of two samples per month per WWTP. Given  
383 the pivotal role of the viral Spike protein in the infectious process, mediating viral entry into  
384 host cells (Jackson et al., 2022) and its significance in generating new VOCs with heightened  
385 transmissibility (Markov et al., 2023), targeted sequencing of the S gene was carried out.

386 The resulting data underwent meticulous analysis to identify diagnostic mutations, low-  
387 frequency mutations, and even new mutations, along with lineage assignment, facilitating  
388 direct comparison with data from clinical surveillance and the data generated in parallel via  
389 the RT-PCR genotyping assays.

390 Throughout the analyses, it became evident that the horizontal coverage of the S gene  
391 varied considerably, significantly impacting the number of mutations detected per sample  
392 (compare Figure 2A with Figure 2C). On average, the S gene's horizontal coverage by at  
393 least 10 reads was  $50.2 \pm 29.5\%$ , with 31% of the samples ( $n = 103$ ) showing coverages  
394 above 70%. However, during specific time points, particularly in weeks encompassing  
395 October and November 2022, and January, March, and April 2023, the horizontal coverage  
396 dropped to an average of less than 25% of the S gene (Figure 2C). Lower coverages also  
397 coincided with higher values of the Simpson Evenness Index. A Simpson Evenness Index  
398 close to 1 indicates that all mutations have equal abundances in the set of samples of that  
399 week, while a value close to 0 suggests the sample set is dominated by only a few highly  
400 prevalent mutations. In our dataset, we observed that lower horizontal coverage of the S  
401 gene led to the detection of fewer mutations per sample, all with more comparable  
402 abundances in the sample set. On the contrary, higher horizontal coverage of the S gene  
403 resulted in the detection of a greater number of mutations per sample, with a few mutations  
404 being over-represented in the samples set. This observation suggests that, in some samples  
405 with low horizontal coverage of the S gene, we might not have been able to capture the full  
406 scope of mutations present.

407 We then attempted to correlate the observed low horizontal coverage of the S gene,  
408 particularly evident in certain weeks (e.g., weeks 39 to 47; Figure 2C), with various  
409 wastewater sample parameters such as the pH, biological oxygen demand, daily  
410 temperature, daily rainfall, and nitrogen and phosphorus concentrations. However, no  
411 significant correlations were found that could explain the observed low S gene coverage  
412 (data not shown). Similarly, no correlations were observed with RNA concentration or viral  
413 load, indicating that other factors might be at play, such as RNA integrity or the presence of  
414 PCR inhibitors commonly found in wastewater samples (Amman et al., 2022; Baaijens et al.,  
415 2021; Silva et al., 2022), despite our additional RNA purification steps. These factors can  
416 adversely affect the sequencing process, leading to limited sequence coverage and  
417 subsequently restricting downstream analysis.

418



419

420 **Figure 2: Number and type of S gene mutations.** **A.** Number of S gene mutations by week. **B.** Box  
 421 plot of the distribution of the Simpson Evenness Index calculated for each analyzed sample and  
 422 represented by week. **C.** Distribution of the average horizontal S gene sequencing coverage  
 423 determined for each sample and represented by week. Horizontal coverage of S gene of at least 10X  
 424 is represented in percentage. **D.** Pie chart showing the relative proportion of each type of mutation  
 425 detected in the samples. STOP refers to a mutation that generates a premature stop codon. **E.** Each  
 426 detected mutation was assigned as being associated with one or multiple lineages based on  
 427 occurrence. Two novel unique mutations were not assigned to any lineage (“No sequences”).

428

429

430 **The majority of detected mutations are missense SNPs associated with the Omicron**  
431 **VOC**

432 In the 332 sequenced samples, a total of 7168 SNPs and 278 insertions/deletions (INDELs)  
433 were discriminated within the S gene over time when compared to the SARS-CoV-2  
434 reference genome (NC\_045512.2). On average, each sample registered  $22 \pm 16$   
435 polymorphisms (comprising both SNPs and INDELs). Among these, the majority were  
436 missense SNPs (89.8%), followed by synonymous SNPs (5.9%), INDELs (3.7%), and the  
437 introduction of premature STOP codons (0.6%) (Figure 2D).

438 The identified missense SNPs were classified based on their occurrence within various  
439 VOCs. Some missense SNPs were associated with one or multiple VOCs, while others were  
440 not specifically linked to any known VOC or had never been previously reported (Figure 2E).  
441 As expected, most missense SNPs were associated with the Omicron VOC (Figure 2E),  
442 which was the dominant VOC in our sampling period. In addition, mutations associated with  
443 older VOCs such as Alpha, Delta, Beta, and Gamma were also sporadically observed in our  
444 samples (Figure 2E). Clinical-derived reports have Delta accounting for 0.01% of worldwide  
445 recovered SARS-CoV-2 sequences during our sampling period (source: GISAID on the 1<sup>st</sup> of  
446 August 2023). Mutations associated with other VOCs, excluding Delta and Omicron, were  
447 sporadic, likely due to their very low prevalence, collectively representing only 0.002% of  
448 worldwide recovered sequences in our sampling period. Note that in the clinical surveillance  
449 data, other VOCs were never detected, which is not surprising given their residual circulation.

450

451 **Frequency and coverage constrain SNP detection in wastewater samples**

452 We proceeded to compare the missense SNPs identified in our wastewater samples with  
453 those detected in clinical samples obtained during the same time period. The aim was to  
454 assess the performance of our wastewater analyses compared to clinical genomic  
455 surveillance. In this analysis, we focused on missense SNPs and found that only 10.7% of

456 them were identified in both sample types - clinical and wastewater (Figure 3A). Most  
457 missense SNPs (61.8%) were exclusively found in clinical-derived sequences, while 27.4%  
458 were exclusively detected in wastewater samples (Figure 3A).

459 Upon closer examination of this distribution, we observed that in weeks where we obtained  
460 higher horizontal coverage of the S gene, the percentage of mutations exclusively found in  
461 clinical samples decreased (Figure 3B).

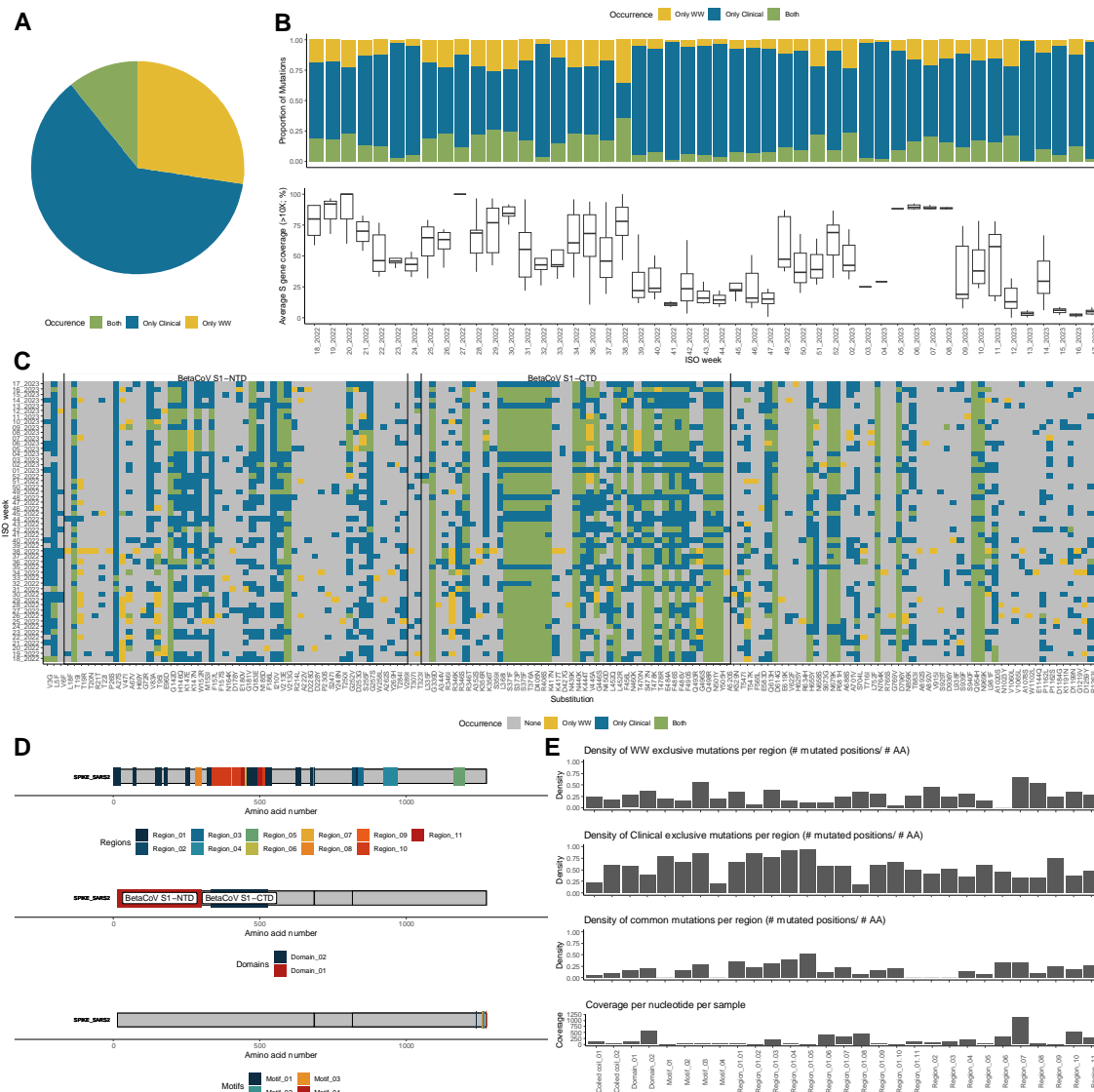
462 We went deeper into our analysis by examining the consistency of detection of missense  
463 mutations present both in clinical and wastewater samples, aiming to identify any patterns  
464 throughout the sampling period and across the full extent of the Spike protein (Figure 3C).

465 We observed three distinct sets of mutations. Firstly, there were mutations that occurred  
466 sporadically in both sample types, such as D228G, K417T, and S929T. These mutations are  
467 of low prevalence, both in Portugal and worldwide (below 1% prevalence as of August 1<sup>st</sup>,  
468 2023, source: outbreak.info). Therefore, their detection in wastewater samples is also  
469 sporadic and not simultaneous with clinical detection. Secondly, there were mutations, such  
470 as S371F, N501Y, and Q954H, that were consistently found in both sample types throughout  
471 the sampling period. These mutations are high frequency mutations (above 50% prevalence  
472 worldwide and in Portugal), making them easier to detect consistently.

473 Lastly, a third set of mutations, e.g., L5F, A27S, and N185D, were frequently found in clinical  
474 samples throughout the sampling period but only sporadically in wastewater samples. These  
475 mutations are also of low frequency but are almost exclusively associated with clinical  
476 samples. During this analysis, we also noticed that many of these mutations occurred in the  
477 BetaCoV\_S1-NTD domain of the Spike protein.

478 We then assessed the density of mutations in each category (exclusive to clinical samples,  
479 exclusive to wastewater samples, or found in both sample types) within the functional and  
480 structural regions of the Spike protein (Figure 3D), taking into account also the horizontal  
481 coverage of each region (Figure 3E). We observed a coverage bias towards specific regions,  
482 particularly the superimposed Domain 2 – BetaCoV S1-CTD, and Region 7. Notably, these  
483 regions are those where we most frequently detect the same mutations in both sample types.

484 Thus, two factors may influence our ability to detect mutations in wastewater samples  
485 through S gene sequencing: the coverage of the S gene and the mutation frequency.  
486



487  
488  
489  
490  
491  
492  
493  
494  
495  
496  
497  
498  
499  
500  
501  
502  
503  
504  
505  
506  
507

**Figure 3: Occurrence of specific missense substitutions.** A. The pie chart shows the relative proportions of substitutions found only in wastewater (WW) samples, only in Clinical samples and in both. B. The top bar plot shows how the relative proportion of missense substitutions found only in WW samples, only in Clinical samples or in both varies per week. The bottom box plots show the distribution of S gene horizontal coverage as in Figure 2C. C. For the set of substitutions that were found in both sample types (i.e., Clinical and WW), the occurrence per week in one of the samples, both or none is shown. D. Spike protein annotation with the Regions, Domains and Motifs analyzed in panel E. E. For each Spike protein Region, Domain, Motif and Coiled coil, the average coverage and the density of mutated positions only found mutated in WW, Clinical, or in both samples, are shown. Region\_01, multiple occurrences of disordered region. Region\_02, putative superantigen; may bind T-cell receptor alpha/TRAC. Region\_03, receptor-binding domain (RBD). Region\_04, integrin-binding motif. Region\_05, receptor-binding motif; binding to human ACE2. Region\_06, immunodominant HLA epitope recognized by the CD8+; called NF9 peptide. Region\_07, putative superantigen; may bind T-cell receptor beta/TRBC1. Region\_08, fusion peptide 1. Region\_09, fusion peptide 2. Region\_10, heptad repeat 1. Region\_11, heptad repeat 2. Domain\_01, BetaCoV S1-NTD. Domain\_02, BetaCoV S1-CTD. Motif\_01, binding to host endocytosis trafficking protein SNX27. Motif\_02, diacidic ER export motif (host COPII). Motif\_03, binding to host plasma membrane localizing/FERM domain proteins. Motif\_04, KxHxx, ER retrieval signal (COPI).

508 **Wastewater sequencing reveals low-frequency mutations missed by clinical**  
509 **surveillance**

510 We then directed our attention to missense SNPs exclusively found in wastewater samples.  
511 Interestingly, other studies have also identified mutations in wastewater that were not  
512 reported in clinical samples collected during the same period (Izquierdo-Lara et al., 2021,  
513 2023; Smyth et al., 2022).

514 First, we investigated in worldwide clinical samples the presence of mutations identified  
515 exclusively in wastewater samples from Portugal and found that all, except two, have been  
516 previously identified, either in Portugal before our sampling period, or in other countries. Two  
517 mutations, G381R and Q607R, were detected in our wastewater samples 11.5 and 9.7  
518 months, respectively, before being reported in Portuguese clinical samples. This highlights  
519 the power of WBS to detect low-frequency mutations, which is due to its intrinsic ability to  
520 sample a large population and capture the underlying viral genetic diversity. Additionally, the  
521 mutations D578E and T998K were never previously detected worldwide, emphasizing WBS's  
522 ability to uncover novel mutations, which could potentially originate from unsampled infected  
523 individuals, viral tropism to different anatomical locations, such as the gastrointestinal tract,  
524 prolonged COVID-19 infection which potentiates in-host evolution, or even an animal  
525 reservoir (Gregory et al., 2022; Smyth et al., 2022).

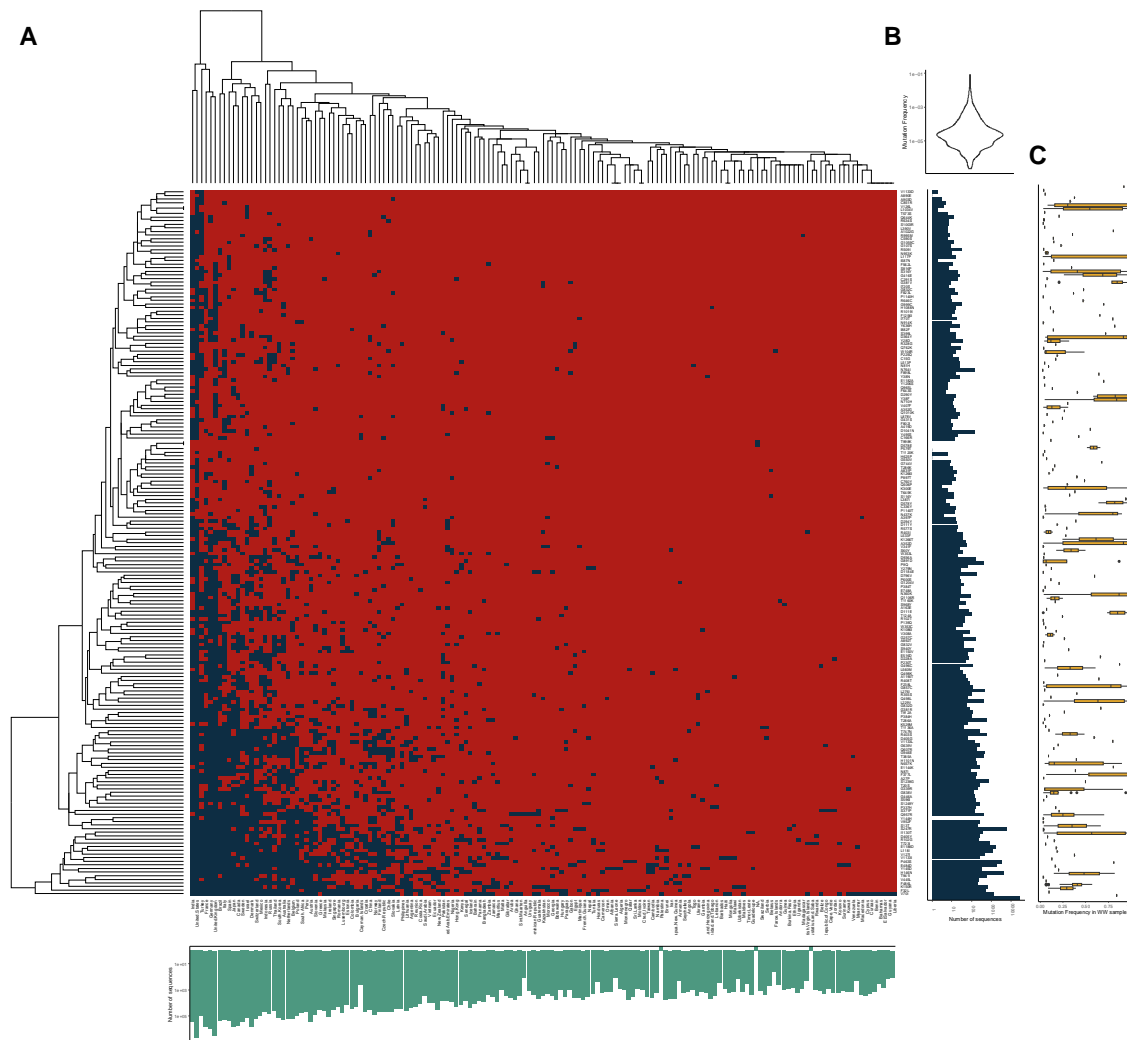
526 We then investigated the distribution of wastewater missense SNPs not detected in our  
527 clinical samples across different countries (Figure 4A). It became apparent that some  
528 mutations emerged in multiple countries, while others were detected only in a few countries  
529 (Figure 4A). The countries with higher numbers of sequenced clinical samples (Figure 4A,  
530 bar chart in green) reported more mutations, and the mutations found at higher frequencies  
531 (Figure 4A, bar chart in blue) were identified across more countries. These results highlight  
532 the influence of mutation frequency on the ability to capture the full extent of viral genetic  
533 diversity and emphasize the importance of sequencing more samples to identify low-  
534 frequency mutations. Note that the mutations detected solely through wastewater S gene  
535 sequencing are present in very low frequencies in clinical samples worldwide (ranging from



536  $2.09 \times 10^{-7}$  to  $8.55 \times 10^{-2}$ ; Figure 4B), whereas they exhibit a diverse frequency range in our  
537 wastewater sample dataset (Figure 4C).

538 These findings highlight the need for an extensive sequencing effort to identify rare  
539 mutations, likely explaining why they have been overlooked in clinical surveillance in  
540 Portugal. It also underscores the importance of comprehensive clinical sampling to detect  
541 such infrequent mutations or alternatively, the adoption of WBS, which can efficiently track  
542 low-frequency mutations by sampling a larger population in one go.

543



544  
545

546 **Figure 4: Amino acid substitution mutations in the S gene only identified in WW samples that**  
547 **were not identified in Portugal's clinical samples.** A. A heat map of occurrence (presence in blue,  
548 absence in red) of each mutation detected in WW samples from Portugal, absent from the clinical  
549 surveillance component in Portugal, but present in clinical samples from countries other than Portugal.  
550 Rows correspond to the mutations and columns to countries. Mutations and countries are sorted by  
551 the mean value of rows and columns, which is reflected in the clustering dendrograms. The green bar  
552 plot on the bottom of the heatmap shows the number of clinical SARS-CoV-2 sequences available for  
553 each country, highlighting the different sequencing efforts of each country. Palestine and Saint  
554 Eustatius and Saba are not considered as independent territories in GISAID, contrary to OutbreakInfo,  
555 and their sequencing efforts are included in Israel and The Netherlands, respectively. The blue bar  
556 plot of the right represents the number of sequences containing the mutation in the set of all available  
557 clinical sequences, highlighting that this set of mutations occurs rarely. B. Violin plot showing the  
558 distribution of the frequencies of these mutations in the represented countries, once again highlighting  
559 that these mutations occur in very low frequencies. C. Box plots representing the frequency of these  
560 mutations in the WWTPs analyzed in this study.  
561

562

563 **The S gene sequencing-based lineage assignment inadequately captures Omicron**  
564 **lineage progression**

565 WBS gained traction during the COVID-19 pandemic, leading to the development of multiple  
566 tools for SARS-CoV-2 lineage assignment from challenging mixed sample sequencing data  
567 (Amman et al., 2022; Karthikeyan et al., 2022; Sapoval et al., 2023). The regular emergence  
568 of new lineages with increasing shared mutations challenges accurate lineage identification  
569 (Fontenele et al., 2021; Izquierdo-Lara et al., 2021; Swift et al., 2022). With over 300  
570 Omicron sub-lineages, high-quality sequencing data becomes increasingly crucial for lineage  
571 assignment.

572 Given our sub-optimal sequencing data of the S gene from mixed samples containing  
573 multiple SARS-CoV-2 lineages, and the low horizontal coverage of a few samples, we  
574 required a robust bioinformatics tool for lineage assignment. Freyja pipeline demonstrated  
575 superior performance compared to other deconvolution methods (Baaijens et al., 2021;  
576 Katharina et al., 2022; Valieris et al., 2022) in terms of accuracy, false-positive rate, and  
577 computational efficiency, making it the selected method for this study.

578 We attempted lineage assignment in all 332 sequenced samples, and the results are  
579 summarized in Figure 1C. The resolution achieved by Freyja was not always sufficient to  
580 make assignments at the level obtained with the RT-PCR genotyping assays, specifically for  
581 the major Omicron lineages, leading to a high frequency of the 'Others' category. The  
582 limitations arise from the low and uneven S-gene horizontal coverage in our samples, with  
583 average values below 25% in several samples, along with the low number of samples  
584 analysed per week (Figure 1D), which collectively hinder the assignment success and the  
585 effective ability to capture the progression of sub-lineages and discriminate within.

586 Nonetheless, the major Omicron sub-lineages circulating in our sampling period (*i.e.*, BA.1.X,  
587 BA.2.X, BA.4.X, BA5.X, and XBB.X) have also been detected. BA.1.X was consistently  
588 present throughout the sampling period (Figure 1C), despite representing a residual  
589 frequency of SARS-CoV-2 infections according to clinical and genotyping assays (Figure 1A  
590 and 1B). BA.2.X was detected throughout the sampling period, gradually decreasing in  
591 frequency, particularly evident after the rise of XBB.X infections in week 5 of 2023. BA.4.X  
592 was always detected, but with higher proportions until week 46 of 2022 (Figure 1C), when it

593 also decreased detection by both genotyping assays and clinical surveillance (Figure 1A and  
594 1B). BA.5.X appeared throughout the sampling period (Figure 1C), aligning with clinical data  
595 as the dominant sub-lineage (Figure 1A). Its frequency gradually reduced with the rise of  
596 XBB.X sub-lineage. XBB.X was first identified by S gene sequencing in week 42 of 2022  
597 (Figure 1C), coinciding with its first detection in clinical data (Figure 1A).

598 The results obtained from S gene sequencing-dependent lineage assignment agree with  
599 genotyping assays and clinical surveillance, but the progression of Omicron sub-lineages is  
600 not well captured by this methodology, likely due to coverage constraints in complex mixed-  
601 samples like wastewater.

602

## 603 **DISCUSSION**

604 Genomic surveillance of SARS-CoV-2 played a crucial role in the COVID-19 pandemic,  
605 providing vital information for understanding virus transmission and evolution, and guiding  
606 effective control measures. However, with the success of vaccination campaigns leading to a  
607 decline in infections and their severity, the focus on genomic surveillance has gradually  
608 decreased worldwide since December 2022, and in Portugal since May 2022, when the  
609 country testing strategy changed. While understandable, given the current impact of the  
610 pandemic, this reduction leaves us unaware of the ongoing infection dynamics and emerging  
611 variants. As a result, more resource-efficient methods like WBS have been explored for  
612 population-wide genomic surveillance. To validate and optimize this new approach, it must  
613 be rigorously compared with current clinical surveillance methods, addressing challenges,  
614 and implementing necessary improvements.

615 Here, we conducted one year of wastewater-based surveillance on the Portuguese  
616 population, spanning from May 2022, when clinical surveillance sequencing efforts began to  
617 decline, until April 2023. The dynamics of SARS-CoV-2 were monitored using a combined  
618 approach of RT-PCR genotyping assays and targeted S gene sequencing.

619 Screening signature Omicron sub-lineage mutations via RT-PCR offers a fast and efficient  
620 method, providing community-level insights and adaptability to emerging mutations, making it

621 a valuable addition to epidemiological surveillance. Moreover, it reduces costs compared to  
622 high-throughput sequencing, enabling broader implementation. However, this approach is  
623 limited to the identification of known sub-lineages with well-known diagnostic mutations and  
624 its discriminatory power diminishes with extensive Omicron VOC diversification. Additionally,  
625 targeted RT-PCR genotyping assays cannot detect new unknown lineages, low frequency  
626 mutations, or novel mutations. They also provide limited information about which variants are  
627 responsible for the overall increase or decrease of SARS-CoV-2 viral load in sewage due to  
628 their inability to determine lineage frequencies in these very complex samples. Thus,  
629 wastewater-based surveillance via RT-PCR genotyping alone cannot fully match the  
630 comprehensive information obtained from clinical genomic surveillance.

631 High-throughput sequencing methods offer significant advantages, providing a broader and  
632 less biased overview of viral genetic diversity and enabling detection of novel lineages,  
633 tracking low-frequency mutations, and identification of mutational hotspots. However, our  
634 data highlights the challenges inherent to wastewater samples, such as biological  
635 complexity, enzymatic inhibitors, viral RNA concentration and integrity, which are critical  
636 factors to obtaining high quality samples required for successful sequencing and full  
637 computational analyses (Izquierdo-Lara et al., 2021). Particularly evident is the impact  
638 introduced by samples in which S gene coverage is low, leading to an underestimation of  
639 mutational diversity and hindering lineage attribution, preventing the full reproduction of the  
640 Omicron sub-lineage succession patterns observed in clinical surveillance. As other authors  
641 already pointed out, in our work, no correlation was found between S gene coverage and  
642 RNA concentration or viral load (Izquierdo-Lara et al., 2021; Pérez-Cataluña et al., 2022),  
643 therefore other parameters such as wastewater storage, pre-process and concentration  
644 before nucleic acid extraction, or biases introduced by library construction and amplicon  
645 sequencing strategies, need to be analysed to infer their impact on RNA recovery and,  
646 consequently, on sequencing performance (Perez-Zabaleta et al., 2023; Tamáš et al., 2022).  
647 Genomics is a rapidly growing field that can yield useful information for public health  
648 surveillance, particularly during ongoing disease outbreaks. Many factors currently affect

649 sequencing quality (e.g. coverage), influencing the full applicability of genomic data. Critical  
650 in the clinical and wastewater contexts is that not all available samples have the same  
651 potential to result in high quality sequencing outcomes, such as genome depth and  
652 coverage. Since horizontal coverage of the S gene may hinder the comprehensive detection  
653 of the wide spectrum of mutations circulating on a given population at the sewershed level, it  
654 is crucial to invest efforts alongside the entire genomics workflow, from sample collection and  
655 sample processing to library construction, sequencing technology and sequence data  
656 analyses, to obtain more accurate and representative outputs. Predictive models of resulting  
657 sequencing depth and coverage based on known variables associated with collected  
658 samples are thus in great demand.

659 The genotyping assays allowed the identification of mutation alleles found in one or more  
660 Omicron sub-lineages, frequently for longer periods compared to the clinical genomic  
661 surveillance data. This time lapse could be attributed to the larger population sampled in  
662 WBS, where one weekly wastewater sample represents up to 920000 people, whereas in  
663 clinical surveillance, an average of 134 persons were sampled per week. It can also reflect  
664 the less biased sampling approach in WBS, which includes both symptomatic and  
665 asymptomatic individuals, and the fact that in clinical surveillance, the presence of the virus  
666 is tested once (usually at the onset of infection), while in WBS it is detected for the full  
667 infection period. During that period, the ongoing excretion of viral RNA in faeces can persist  
668 approximately for an average duration of 14-21 days (Lescure et al., 2020; Pan et al., 2020),  
669 with SARS-CoV-2 shedding having been reported for up to 55 days in patients with  
670 complications or admitted to intensive care units (Lavania et al., 2022).

671 Another relevant aspect of our analysis concerns low-frequency mutations, including two that  
672 were first detected in wastewater samples and much later in clinical samples, and two  
673 mutations never previously reported worldwide. This is in line with other wastewater  
674 sequencing surveillance initiatives, where mutations in Spike were identified months before  
675 being reported in clinical samples (Izquierdo-Lara et al., 2023; La Rosa et al., 2023; Pérez-  
676 Cataluña et al., 2022), highlighting the potential of wastewater surveillance as an early

677 warning system. For example, and considering the most recent variant of interest EG.5, a  
678 descendent of XBB.1.X (risk evaluation from 9 August 2023, by WHO), this lineage was  
679 identified in very low-frequency in our wastewater samples from week 16 of 2023, however it  
680 was reported on clinical data only from week 18 onward, re-enforcing the capability of WBS  
681 to anticipate trends and upsurges in a given region.

682 Early detection of low-frequency mutations is crucial to monitor the evolution of SARS-CoV-  
683 2, as they serve as the basis for natural selection and can give rise to new VOCs/lineages  
684 that may be more transmissible or cause more severe infections. We observed that several  
685 low-frequency mutations were detected in clinical samples but not in wastewater samples,  
686 likely due to their low frequency, making their detection more random in either sample type.  
687 On the contrary, we also found several mutations in wastewater samples that were not  
688 previously seen in Portugal through clinical surveillance. Similar findings were also made by  
689 Pérez-Cataluna and collaborators in Spain, and La Rosa and collaborators in Italy, with the  
690 report of exclusive wastewater mutations or mutations not reported as dominant in clinical  
691 samples (La Rosa et al., 2023; Pérez-Cataluña et al., 2022). The report of novel amino acid  
692 substitutions at Spike gene were also reported in other publications (Crits-Christoph et al.,  
693 2021; Pérez-Cataluña et al., 2021; Smyth et al., 2022).

694 The low-frequency and novel mutations may originate from unsampled individuals, which is  
695 not unlikely given that our sampling period corresponds to the time point in which clinical  
696 surveillance decreased in Portugal. They can also originate from asymptomatic cases,  
697 viruses replicating in different body sites (e.g., respiratory vs. gastrointestinal tracts),  
698 prolonged infections leading to in-host evolution, or even from animal reservoirs whose  
699 excretions also end up in the same wastewater treatment plants (Gregory et al., 2022; Smyth  
700 et al., 2022).

701 Although not able to completely replace clinical surveillance, allelic discrimination assays and  
702 S gene sequencing can complement each other to overcome their respective limitations. We  
703 envision an implementation scheme in which the RT-PCR genotyping assays, selected  
704 based on the data being collected weekly and by the sequencing results, allow fast testing of

705 a large number of samples, covering a very large set of the population. Additionally,  
706 successful implementation of S gene targeted sequencing in parallel will allow regular  
707 monitoring of virus evolution and detection, and tracking low-frequency mutations.

708

## 709 **CONCLUSION**

710 In summary, the combination of wastewater genomic surveillance using RT-PCR assays and  
711 S gene sequencing provided useful insights into the diversity of circulating Omicron sub-  
712 lineages within the sampled population throughout 12 months. Although each method has its  
713 own limitations in terms of lineage discrimination, when used together, they offer a reliable  
714 snapshot of the local epidemiological situation. Additionally, this combined approach enables  
715 fast lineage attribution alongside the identification of low-frequency and novel mutations,  
716 which would typically require extensive clinical sampling and sequencing efforts. Further,  
717 they support the prolonged detection of lineages considered by clinical surveillance to be  
718 already out of circulation. The results generated in this work evidence the value of  
719 environmental surveillance to capture public health trends and underscore the effectiveness  
720 of WBS as a tracking system for virus variants. Moreover, WBS offers the opportunity to  
721 transform the cost per clinical sample into the cost per sewershed.

722 In conclusion, our findings emphasize that knowledge of the genetic diversity of SARS-CoV-2  
723 at the population level can be extended far beyond via the combination of routine clinical  
724 genomic surveillance with wastewater sequencing and genotyping.

725

## 726 **ACKNOWLEDGMENTS**

727 We acknowledge the coordination efforts of AdP VALOR from the very first moment,  
728 particularly of Ana Katila Ribeiro, Marta Carvalho and Nuno Brôco, and the engagement of  
729 the Portuguese Environment Agency [APA] and the National Health Authority [DGS] as well,  
730 in setting up a national surveillance system. Thanks are due to Anabela Rebelo [APA].

731 We acknowledge the close collaboration of water utilities [AGERE, Águas do Algarve, Águas  
732 do Centro Litoral, Águas do Norte, Águas do Tejo Atlântico, Águas e Energia do Porto,



733 SIMDOURO, SMAS Almada] along this project and thank all their employees who  
734 contributed to wastewater sampling.

735 The institutional support of *Ministério do Ambiente e Ação Climática* and the European  
736 Commission's *DG Joint Research Centre*, Directorate D – Sustainable Resources is  
737 gratefully acknowledged.

738

### 739 **FUNDING**

740 This work was supported by the European Union through the Emergency Support Instrument  
741 [*Support to the Member States to establish national systems, local collection points, and*  
742 *digital infrastructure for monitoring Covid19 and its variants in wastewater – Portugal*; Grant  
743 Agreement No. 060701/2021/864489/SUB/ENV.C2], Fundo Ambiental (MAAC), and  
744 Fundação para a Ciência e a Tecnologia, IP [institutional support to cE3c  
745 (UIDB/00329/2020); BiolSI (UIDB/04046/2020); and CHANGE (LA/P/0121/2020)].

746

### 747 **CONFLICTS OF INTEREST**

748 The authors declare no conflict of interest. The funders had no role in the design of the study;  
749 in the collection, analyses, or interpretation of data; in the writing of the manuscript, or in the  
750 decision to publish the results.

751

### 752 **DATA AND MATERIALS AVAILABILITY**

753 Materials generated in this study will be made available upon request. All data needed to  
754 evaluate the conclusions of this work are present in the paper and/or the Supplementary  
755 Materials. This paper does not report original code. Any additional information required to  
756 reanalyse the data reported in this paper is available from the lead contact upon request.

757

### 758 **SUPPLEMENTARY MATERIALS**

759 We provide supplementary files with supporting material, including Supplementary Table 1  
760 and Supplementary Figures 1 to 5 (Figures S1-S5).

761

762

## 763 REFERENCES

- 764 Afgan, E., Baker, D., Batut, B., van den Beek, M., Bouvier, D., Cech, M., Chilton, J., Clements, D.,  
765 Coraor, N., Grüning, B.A., Guerler, A., Hillman-Jackson, J., Hiltemann, S., Jalili, V., Rasche, H.,  
766 Soranzo, N., Goecks, J., Taylor, J., Nekrutenko, A., Blankenberg, D., 2018. The Galaxy platform  
767 for accessible, reproducible and collaborative biomedical analyses: 2018 update. *Nucleic*  
768 *Acids Res.* 46, W537–W544. <https://doi.org/10.1093/nar/gky379>
- 769 Agrawal, S., Orschler, L., Lackner, S., 2021. Long-term monitoring of SARS-CoV-2 RNA in wastewater  
770 of the Frankfurt metropolitan area in Southern Germany. *Sci. Rep.* 11, 5372.  
771 <https://doi.org/10.1038/s41598-021-84914-2>
- 772 Alkuzweny, M., Gangavarapu, K., Hughes, L., 2023. outbreak.info R Client [WWW Document]. URL  
773 <https://outbreak-info.github.io/R-outbreak-info/> (accessed 8.8.23).
- 774 Amman, F., Markt, R., Endler, L., Hupfau, S., Agerer, B., Schedl, A., Richter, L., Zechmeister, M.,  
775 Bicher, M., Heiler, G., Triska, P., Thornton, M., Penz, T., Senekowitsch, M., Laine, J., Keszei, Z.,  
776 Klimek, P., Nägele, F., Mayr, M., Daleiden, B., Steinlechner, M., Niederstätter, H., Heidinger,  
777 P., Rauch, W., Scheffknecht, C., Vogl, G., Weichlinger, G., Wagner, A.O., Slipko, K., Masseron,  
778 A., Radu, E., Allerberger, F., Popper, N., Bock, C., Schmid, D., Oberacher, H., Kreuzinger, N.,  
779 Insam, H., Bergthaler, A., 2022. Viral variant-resolved wastewater surveillance of SARS-CoV-2  
780 at national scale. *Nat. Biotechnol.* 40, 1814–1822. [https://doi.org/10.1038/s41587-022-](https://doi.org/10.1038/s41587-022-01387-y)  
781 [01387-y](https://doi.org/10.1038/s41587-022-01387-y)
- 782 Auguie, B., Antonov, A., 2017. gridExtra: Miscellaneous Functions for “Grid” Graphics.
- 783 Baaijens, J.A., Zulli, A., Ott, I.M., Petrone, M.E., Alpert, T., Fauver, J.R., Kalinich, C.C., Vogels, C.B.F.,  
784 Breban, M.I., Duvallet, C., McElroy, K., Ghaeli, N., Imakaev, M., Mckenzie-Bennett, M.,  
785 Robison, K., Plocik, A., Schilling, R., Pierson, M., Littlefield, R., Spencer, M., Simen, B.B.,  
786 Hanage, W.P., Grubaugh, N.D., Peccia, J., Baym, M., 2021. Variant abundance estimation for  
787 SARS-CoV-2 in wastewater using RNA-Seq quantification. *medRxiv* 2021.08.31.21262938.  
788 <https://doi.org/10.1101/2021.08.31.21262938>
- 789 Bar-Or, I., Weil, M., Indenbaum, V., Bucris, E., Bar-Ilan, D., Elul, M., Levi, N., Aguvaev, I., Cohen, Z.,  
790 Shirazi, R., Erster, O., Sela-Brown, A., Sofer, D., Mor, O., Mendelson, E., Zuckerman, N.S.,  
791 2021. Detection of SARS-CoV-2 variants by genomic analysis of wastewater samples in Israel.  
792 *Sci. Total Environ.* 789, 148002. <https://doi.org/10.1016/j.scitotenv.2021.148002>
- 793 Bittinger, K., 2020. abdiv: Alpha and Beta Diversity Measures.
- 794 Bolger, A.M., Lohse, M., Usadel, B., 2014. Trimmomatic: a flexible trimmer for Illumina sequence  
795 data. *Bioinformatics* 30, 2114–2120. <https://doi.org/10.1093/bioinformatics/btu170>
- 796 Brennan, P., 2018. drawProteins: a Bioconductor/R package for reproducible and programmatic  
797 generation of protein schematics. *F1000Research* 7, 1105.
- 798 Cingolani, P., Platts, A., Wang, L.L., Coon, M., Nguyen, T., Wang, L., Land, S.J., Lu, X., Ruden, D.M.,  
799 2012. A program for annotating and predicting the effects of single nucleotide  
800 polymorphisms, SnpEff. *Fly (Austin)* 6, 80–92. <https://doi.org/10.4161/fly.19695>
- 801 Commission Recommendation (EU) 2021/472 (European Commission Recommendation (EU)  
802 2021/472 of 17 March 2021 on a common approach to establish a systematic surveillance of  
803 SARS-CoV-2 and its variants in wastewaters in the EU), 2021. , OJ L. European Commission.
- 804 Corman, V.M., Landt, O., Kaiser, M., Molenkamp, R., Meijer, A., Chu, D.K., Bleicker, T., Brünink, S.,  
805 Schneider, J., Schmidt, M.L., Mulders, D.G., Haagmans, B.L., van der Veer, B., van den Brink,  
806 S., Wijsman, L., Goderski, G., Romette, J.-L., Ellis, J., Zambon, M., Peiris, M., Goossens, H.,  
807 Reusken, C., Koopmans, M.P., Drosten, C., 2020. Detection of 2019 novel coronavirus (2019-  
808 nCoV) by real-time RT-PCR. *Eurosurveillance* 25, 2000045. [https://doi.org/10.2807/1560-](https://doi.org/10.2807/1560-7917.ES.2020.25.3.2000045)  
809 [7917.ES.2020.25.3.2000045](https://doi.org/10.2807/1560-7917.ES.2020.25.3.2000045)

- 810 Crits-Christoph, A., Kantor, R.S., Olm, M.R., Whitney, O.N., Al-Shayeb, B., Lou, Y.C., Flamholz, A.,  
811 Kennedy, L.C., Greenwald, H., Hinkle, A., Hetzel, J., Spitzer, S., Koble, J., Tan, A., Hyde, F.,  
812 Schroth, G., Kuersten, S., Banfield, J.F., Nelson, K.L., 2021. Genome Sequencing of Sewage  
813 Detects Regionally Prevalent SARS-CoV-2 Variants. *mBio* 12, e02703-20.  
814 <https://doi.org/10.1128/mBio.02703-20>
- 815 Elbe, S., Buckland-Merrett, G., 2017. Data, disease and diplomacy: GISAID's innovative contribution  
816 to global health. *Glob. Chall.* 1, 33–46. <https://doi.org/10.1002/gch2.1018>
- 817 Elsamadony, M., Fujii, M., Miura, T., Watanabe, T., 2021. Possible transmission of viruses from  
818 contaminated human feces and sewage: Implications for SARS-CoV-2. *Sci. Total Environ.* 755,  
819 142575. <https://doi.org/10.1016/j.scitotenv.2020.142575>
- 820 Foladori, P., Cutrupi, F., Segata, N., Manara, S., Pinto, F., Malpei, F., Bruni, L., La Rosa, G., 2020. SARS-  
821 CoV-2 from faeces to wastewater treatment: What do we know? A review. *Sci. Total Environ.*  
822 743, 140444. <https://doi.org/10.1016/j.scitotenv.2020.140444>
- 823 Fontenele, R.S., Kraberger, S., Hadfield, J., Driver, E.M., Bowes, D., Holland, L.A., Faleye, T.O.C.,  
824 Adhikari, S., Kumar, R., Inchausti, R., Holmes, W.K., Deitrick, S., Brown, P., Duty, D., Smith, T.,  
825 Bhatnagar, A., Yeager, R.A., Holm, R.H., von Reitzenstein, N.H., Wheeler, E., Dixon, K.,  
826 Constantine, T., Wilson, M.A., Lim, E.S., Jiang, X., Halden, R.U., Scotch, M., Varsani, A., 2021.  
827 High-throughput sequencing of SARS-CoV-2 in wastewater provides insights into circulating  
828 variants. *MedRxiv Prepr. Serv. Health Sci.* 2021.01.22.21250320.  
829 <https://doi.org/10.1101/2021.01.22.21250320>
- 830 Galani, A., Aalizadeh, R., Kostakis, M., Markou, A., Alygizakis, N., Lytras, T., Adamopoulos, P.G.,  
831 Peccia, J., Thompson, D.C., Kontou, A., Karagiannidis, A., Lianidou, E.S., Avgeris, M.,  
832 Paraskevis, D., Tsiodras, S., Scorilas, A., Vasiliou, V., Dimopoulos, M.-A., Thomaidis, N.S.,  
833 2022. SARS-CoV-2 wastewater surveillance data can predict hospitalizations and ICU  
834 admissions. *Sci. Total Environ.* 804, 150151. <https://doi.org/10.1016/j.scitotenv.2021.150151>
- 835 Gangavarapu, K., Latif, A.A., Mullen, J.L., Alkuzweny, M., Hufbauer, E., Tsueng, G., Haag, E., Zeller, M.,  
836 Aceves, C.M., Zaiets, K., Cano, M., Zhou, X., Qian, Z., Sattler, R., Matteson, N.L., Levy, J.I., Lee,  
837 R.T.C., Freitas, L., Maurer-Stroh, S., Suchard, M.A., Wu, C., Su, A.I., Andersen, K.G., Hughes,  
838 L.D., 2023. Outbreak.info genomic reports: scalable and dynamic surveillance of SARS-CoV-2  
839 variants and mutations. *Nat. Methods* 20, 512–522. [https://doi.org/10.1038/s41592-023-](https://doi.org/10.1038/s41592-023-01769-3)  
840 [01769-3](https://doi.org/10.1038/s41592-023-01769-3)
- 841 Gregory, D.A., Trujillo, M., Rushford, C., Flury, A., Kannyo, S., San, K.M., Lyfoung, D., Wiseman, R.W.,  
842 Bromert, K., Zhou, M.-Y., Kesler, E., Bivens, N., Hoskins, J., Lin, C.-H., O'Connor, D.H.,  
843 Wieberg, C., Wenzel, J., Kantor, R.S., Dennehy, J.J., Johnson, M.C., 2022. Genetic Diversity  
844 and Evolutionary Convergence of Cryptic SARS-CoV-2 Lineages Detected Via Wastewater  
845 Sequencing. *MedRxiv Prepr. Serv. Health Sci.* 2022.06.03.22275961.  
846 <https://doi.org/10.1101/2022.06.03.22275961>
- 847 Grubaugh, N.D., Gangavarapu, K., Quick, J., Matteson, N.L., De Jesus, J.G., Main, B.J., Tan, A.L., Paul,  
848 L.M., Brackney, D.E., Grewal, S., Gurfield, N., Van Rompay, K.K.A., Isern, S., Michael, S.F.,  
849 Coffey, L.L., Loman, N.J., Andersen, K.G., 2019. An amplicon-based sequencing framework for  
850 accurately measuring intrahost virus diversity using PrimalSeq and iVar. *Genome Biol.* 20, 8.  
851 <https://doi.org/10.1186/s13059-018-1618-7>
- 852 Harris, C.R., Millman, K.J., van der Walt, S.J., Gommers, R., Virtanen, P., Cournapeau, D., Wieser, E.,  
853 Taylor, J., Berg, S., Smith, N.J., Kern, R., Picus, M., Hoyer, S., van Kerkwijk, M.H., Brett, M.,  
854 Haldane, A., del Río, J.F., Wiebe, M., Peterson, P., Gérard-Marchant, P., Sheppard, K., Reddy,  
855 T., Weckesser, W., Abbasi, H., Gohlke, C., Oliphant, T.E., 2020. Array programming with  
856 NumPy. *Nature* 585, 357–362. <https://doi.org/10.1038/s41586-020-2649-2>
- 857 INSA, 2021. Diversidade genética do novo coronavírus SARS-CoV-2 (COVID-19) em Portugal [WWW  
858 Document]. *Divers. Genética Novo Coronavírus SARS-CoV-2 COVID-19 Em Port.* URL  
859 <https://insaflu.insa.pt/covid19/>
- 860 Izquierdo-Lara, R., Elsinga, G., Heijnen, L., Munnink, B.B.O., Schapendonk, C.M.E., Nieuwenhuijse, D.,  
861 Kon, M., Lu, L., Aarestrup, F.M., Lycett, S., Medema, G., Koopmans, M.P.G., de Graaf, M.,

- 862 2021. Monitoring SARS-CoV-2 Circulation and Diversity through Community Wastewater  
863 Sequencing, the Netherlands and Belgium. *Emerg. Infect. Dis.* 27, 1405–1415.  
864 <https://doi.org/10.3201/eid2705.204410>
- 865 Izquierdo-Lara, R.W., Heijnen, L., Oude Munnink, B.B., Schapendonk, C.M.E., Elsinga, G., Langeveld, J.,  
866 Post, J., Prasad, D.K., Carrizosa, C., Been, F., van Beek, J., Schilperoort, R., Vriend, R., Fanoy,  
867 E., de Schepper, E.I.T., Sikkema, R.S., Molenkamp, R., Aarestrup, F.M., Medema, G.,  
868 Koopmans, M.P.G., de Graaf, M., 2023. Rise and fall of SARS-CoV-2 variants in Rotterdam:  
869 Comparison of wastewater and clinical surveillance. *Sci. Total Environ.* 873, 162209.  
870 <https://doi.org/10.1016/j.scitotenv.2023.162209>
- 871 Jackson, C.B., Farzan, M., Chen, B., Choe, H., 2022. Mechanisms of SARS-CoV-2 entry into cells. *Nat.*  
872 *Rev. Mol. Cell Biol.* 23, 3–20. <https://doi.org/10.1038/s41580-021-00418-x>
- 873 Karthikeyan, S., Levy, J.I., De Hoff, P., Humphrey, G., Birmingham, A., Jepsen, K., Farmer, S., Tubb,  
874 H.M., Valles, T., Tribelhorn, C.E., Tsai, R., Aigner, S., Sathe, S., Moshiri, N., Henson, B., Mark,  
875 A.M., Hakim, A., Baer, N.A., Barber, T., Belda-Ferre, P., Chacón, M., Cheung, W., Cresini, E.S.,  
876 Eisner, E.R., Lastrella, A.L., Lawrence, E.S., Marotz, C.A., Ngo, T.T., Ostrander, T., Plascencia,  
877 A., Salido, R.A., Seaver, P., Smoot, E.W., McDonald, D., Neuhaard, R.M., Scioscia, A.L.,  
878 Satterlund, A.M., Simmons, E.H., Abelman, D.B., Brenner, D., Bruner, J.C., Buckley, A., Ellison,  
879 M., Gattas, J., Gonias, S.L., Hale, M., Hawkins, F., Ikeda, L., Jhaveri, H., Johnson, T., Kellen, V.,  
880 Kremer, B., Matthews, G., McLawhon, R.W., Ouillet, P., Park, D., Pradenas, A., Reed, S., Riggs,  
881 L., Sanders, A., Sollenberger, B., Song, A., White, B., Winbush, T., Aceves, C.M., Anderson,  
882 Catelyn, Gangavarapu, K., Hufbauer, E., Kurzban, E., Lee, J., Matteson, N.L., Parker, E.,  
883 Perkins, S.A., Ramesh, K.S., Robles-Sikisaka, R., Schwab, M.A., Spencer, E., Wohl, S.,  
884 Nicholson, L., McHardy, I.H., Dimmock, D.P., Hobbs, C.A., Bakhtar, O., Harding, A., Mendoza,  
885 A., Bolze, A., Becker, D., Cirulli, E.T., Isaksson, M., Schiabor Barrett, K.M., Washington, N.L.,  
886 Malone, J.D., Schafer, A.M., Gurfield, N., Stous, S., Fielding-Miller, R., Garfein, R.S., Gaines, T.,  
887 Anderson, Cheryl, Martin, N.K., Schooley, R., Austin, B., MacCannell, D.R., Kingsmore, S.F.,  
888 Lee, W., Shah, S., McDonald, E., Yu, A.T., Zeller, M., Fisch, K.M., Longhurst, C., Maysent, P.,  
889 Pride, D., Khosla, P.K., Laurent, L.C., Yeo, G.W., Andersen, K.G., Knight, R., 2022. Wastewater  
890 sequencing reveals early cryptic SARS-CoV-2 variant transmission. *Nature* 609, 101–108.  
891 <https://doi.org/10.1038/s41586-022-05049-6>
- 892 Katharina, J., David, D., Ivan, T., Anina, K., Pravin, G., Xavier, F.-C., Carola, B., Alexander, D., Elyse, S.,  
893 Lea, C., Fedderica, C., Alex, C., Lara, F., Chaoran, C., Kim, J., Sarah, N., Mirjam, F., Christian, B.,  
894 Catharine, A., Tanja, S., Christoph, O., Tamar, K., Timothy, J., Niko, B., 2022. Early detection  
895 and surveillance of SARS-CoV-2 genomic variants in wastewater using COJAC. *Nat. Microbiol.*  
896 7. <https://doi.org/10.1038/s41564-022-01185-x>
- 897 Khateeb, J., Li, Y., Zhang, H., 2021. Emerging SARS-CoV-2 variants of concern and potential  
898 intervention approaches. *Crit. Care* 25, 244. <https://doi.org/10.1186/s13054-021-03662-x>
- 899 Kuzmina, A., Wattad, S., Engel, S., Rosenberg, E., Taube, R., 2022. Functional Analysis of Spike from  
900 SARS-CoV-2 Variants Reveals the Role of Distinct Mutations in Neutralization Potential and  
901 Viral Infectivity. *Viruses* 14, 803. <https://doi.org/10.3390/v14040803>
- 902 La Rosa, G., Brandtner, D., Bonanno Ferraro, G., Veneri, C., Mancini, P., Iaconelli, M., Lucentini, L., Del  
903 Giudice, C., Orlandi, L., Palma, A., Calabria, A., Carnevali, A., Nehludoff, A., Stenico, A., Izzotti,  
904 A., Barca, A., Tosco, A., Porta, A., Lombardi, A., Voli, A., Franzetti, A., Ciccaglione, A., Costa,  
905 A., D’Argenzio, A., Romano, A., Pariani, A., Carducci, A., Grucci, A., Prast, A.-M., Agodi, A.,  
906 Cersini, A., Giorgi, A., Bertasi, B., Griglio, B., Ancona, C., Maida, C.M., Montanaro, C., Filizzolo,  
907 C., Ottaviano, C., Cocuzza, C., Pignata, C., Nasci, D., Cereda, D., Oliva, D., Giorgi, D.A.,  
908 Malacaria, E., Grasselli, E., Nicosia, E., Carraro, E., Ammoni, E., Grange, E., Federici, E.,  
909 Filippetti, F., Tramuto, F., Guarneri, F., Serio, F., Damasco, F., Palumbo, F., Apollonio, F.,  
910 Cutrupi, F., Gucciardi, F., Pennino, F., Russo, F., Triggiano, F., Rigoli, F., Pietrella, G., Trani, G.,  
911 Rossolini, G.M., Bulotta, G., Fusco, G., La Vecchia, G., Alborali, G., Giammanco, G., Santoro,  
912 G., Pitter, G., Purpari, G., Aprea, G., Di Vittorio, G., Folino, G., Lauria, G., Federigi, I., Amoruso,  
913 I., Ferrante, I., Tomesani, I., De Lellis, L., Pellegrinelli, L., Demetz, L., Gentili, L., Richiardi, L.,

- 914 Zago, L., Masieri, L., Decastelli, L., Bolognini, L., Cossentino, L., Bianchi, M., Verani, M.,  
915 Zampini, M., Ferrante, M., Cadonna, M., Montagna, M.T., Scicluna, M.T., Arizzi, M., Mariuz,  
916 M., Palermo, M., Bellisomi, M., Paniccà, M., Barchitta, M., Ramazzotti, M., Postinghel, M.,  
917 Viscardi, M., Ruffier, M., Petricciuolo, M., La Bianca, M., Colitti, M., Monfrinotti, M., Fontani,  
918 N., Formenti, N., Mongelli, O., De Giglio, O., Angelini, P., Foladori, P., Torlontano, P., Calà, P.,  
919 Cifarelli, R.A., Binda, S., Briscolini, S., Castiglioni, S., Bonetta, S., Magi, S., Scattolini, S.,  
920 Schiarea, S., De Grazia, S., Rosatto, S., Baldovin, T., Primache, V., Groppi, V., Acciari, V.A.,  
921 Mazzucco, W., Suffredini, E., 2023. Wastewater surveillance of SARS-CoV-2 variants in  
922 October–November 2022 in Italy: detection of XBB.1, BA.2.75 and rapid spread of the BQ.1  
923 lineage. *Sci. Total Environ.* 873, 162339. <https://doi.org/10.1016/j.scitotenv.2023.162339>
- 924 Lavania, M., Joshi, M.S., Ranshing, S.S., Potdar, V.A., Shinde, M., Chavan, N., Jadhav, S.M., Sarkale, P.,  
925 Mohandas, S., Sawant, P.M., Tikute, S., Padbidri, V., Patwardhan, S., Kate, R., 2022.  
926 Prolonged Shedding of SARS-CoV-2 in Feces of COVID-19 Positive Patients: Trends in  
927 Genomic Variation in First and Second Wave. *Front. Med.* 9.
- 928 Lescure, F.-X., Bouadma, L., Nguyen, D., Parisey, M., Wicky, P.-H., Behillil, S., Gaynard, A.,  
929 Bouscambert-Duchamp, M., Donati, F., Le Hingrat, Q., Enouf, V., Houhou-Fidouh, N., Valette,  
930 M., Mailles, A., Lucet, J.-C., Mentre, F., Duval, X., Descamps, D., Malvy, D., Timsit, J.-F., Lina,  
931 B., van-der-Werf, S., Yazdanpanah, Y., 2020. Clinical and virological data of the first cases of  
932 COVID-19 in Europe: a case series. *Lancet Infect. Dis.* 20, 697–706.  
933 [https://doi.org/10.1016/S1473-3099\(20\)30200-0](https://doi.org/10.1016/S1473-3099(20)30200-0)
- 934 Li, H., 2013. Aligning sequence reads, clone sequences and assembly contigs with BWA-MEM.  
935 <https://doi.org/10.48550/arXiv.1303.3997>
- 936 Markov, P.V., Ghafari, M., Beer, M., Lythgoe, K., Simmonds, P., Stilianakis, N.I., Katzourakis, A., 2023.  
937 The evolution of SARS-CoV-2. *Nat. Rev. Microbiol.* 21, 361–379.  
938 <https://doi.org/10.1038/s41579-023-00878-2>
- 939 McKinney, W., 2010. Data Structures for Statistical Computing in Python. Presented at the  
940 Proceedings of the 9th Python in Science Conference, Austin, Texas, pp. 51–56.  
941 <https://doi.org/10.25080/Majora-92bf1922-00a>
- 942 Medema, G., Heijnen, L., Elsinga, G., Italiaander, R., Brouwer, A., 2020. Presence of SARS-  
943 Coronavirus-2 RNA in Sewage and Correlation with Reported COVID-19 Prevalence in the  
944 Early Stage of the Epidemic in The Netherlands. *Environ. Sci. Technol. Lett.*  
945 *acs.estlett.0c00357*. <https://doi.org/10.1021/acs.estlett.0c00357>
- 946 Monteiro, S., Rente, D., Cunha, M.V., Gomes, M.C., Marques, T.A., Lourenço, A.B., Cardoso, E.,  
947 Álvaro, P., Silva, M., Coelho, N., Vilaça, J., Meireles, F., Brôco, N., Carvalho, M., Santos, R.,  
948 2022. A wastewater-based epidemiology tool for COVID-19 surveillance in Portugal. *Sci. Total*  
949 *Environ.* 804, 150264. <https://doi.org/10.1016/j.scitotenv.2021.150264>
- 950 Morgan, M., Ramos, M., 2023. BiocManager: Access the Bioconductor Project Package Repository.
- 951 Nemudryi, A., Nemudraia, A., Wiegand, T., Surya, K., Buyukyoruk, M., Cicha, C., Vanderwood, K.K.,  
952 Wilkinson, R., Wiedenheft, B., 2020. Temporal Detection and Phylogenetic Assessment of  
953 SARS-CoV-2 in Municipal Wastewater. *Cell Rep. Med.* 1, 100098.  
954 <https://doi.org/10.1016/j.xcrm.2020.100098>
- 955 Nkambule, S., Johnson, R., Mathee, A., Mahlangeni, N., Webster, C., Horn, S., Mangwana, N., Dias, S.,  
956 Sharma, J.R., Ramharack, P., Louw, J., Reddy, T., Surujlal-Naicker, S., Mdhluli, M., Gray, G.,  
957 Muller, C., Street, R., 2023. Wastewater-based SARS-CoV-2 airport surveillance: key trends at  
958 the Cape Town International Airport. *J. Water Health* 21, 402–408.  
959 <https://doi.org/10.2166/wh.2023.281>
- 960 Okonechnikov, K., Conesa, A., García-Alcalde, F., 2016. Qualimap 2: advanced multi-sample quality  
961 control for high-throughput sequencing data. *Bioinforma. Oxf. Engl.* 32, 292–294.  
962 <https://doi.org/10.1093/bioinformatics/btv566>
- 963 Pan, Y., Zhang, D., Yang, P., Poon, L.L.M., Wang, Q., 2020. Viral load of SARS-CoV-2 in clinical samples.  
964 *Lancet Infect. Dis.* 20, 411–412. [https://doi.org/10.1016/S1473-3099\(20\)30113-4](https://doi.org/10.1016/S1473-3099(20)30113-4)

- 965 Peccia, J., Zulli, A., Brackney, D.E., Grubaugh, N.D., Kaplan, E.H., Casanovas-Massana, A., Ko, A.I.,  
966 Malik, A.A., Wang, D., Wang, M., Warren, J.L., Weinberger, D.M., Arnold, W., Omer, S.B.,  
967 2020. Measurement of SARS-CoV-2 RNA in wastewater tracks community infection dynamics.  
968 *Nat. Biotechnol.* 38, 1164–1167. <https://doi.org/10.1038/s41587-020-0684-z>
- 969 Pedersen, T.L., 2022. ggforce: Accelerating “ggplot2.”
- 970 Pérez-Cataluña, A., Chiner-Oms, Á., Cuevas-Ferrando, E., Díaz-Reolid, A., Falcó, I., Randazzo, W.,  
971 Girón-Guzmán, I., Allende, A., Bracho, M.A., Comas, I., Sánchez, G., 2022. Spatial and  
972 temporal distribution of SARS-CoV-2 diversity circulating in wastewater. *Water Res.* 211,  
973 118007. <https://doi.org/10.1016/j.watres.2021.118007>
- 974 Pérez-Cataluña, A., Cuevas-Ferrando, E., Randazzo, W., Falcó, I., Allende, A., Sánchez, G., 2021.  
975 Comparing analytical methods to detect SARS-CoV-2 in wastewater. *Sci. Total Environ.* 758,  
976 143870. <https://doi.org/10.1016/j.scitotenv.2020.143870>
- 977 Perez-Zabaleta, M., Archer, A., Khatami, K., Jafferli, M.H., Nandy, P., Atasoy, M., Birgersson, M.,  
978 Williams, C., Cetecioglu, Z., 2023. Long-term SARS-CoV-2 surveillance in the wastewater of  
979 Stockholm: What lessons can be learned from the Swedish perspective? *Sci. Total Environ.*  
980 858, 160023. <https://doi.org/10.1016/j.scitotenv.2022.160023>
- 981 R Core Team, 2021. R: The R Project for Statistical Computing [WWW Document]. *Lang. Environ. Stat.*  
982 *Comput.* URL <https://www.r-project.org/> (accessed 8.8.23).
- 983 Rambaut, A., Holmes, E.C., O’Toole, Á., Hill, V., McCrone, J.T., Ruis, C., du Plessis, L., Pybus, O.G.,  
984 2020. A dynamic nomenclature proposal for SARS-CoV-2 lineages to assist genomic  
985 epidemiology. *Nat. Microbiol.* 5, 1403–1407. <https://doi.org/10.1038/s41564-020-0770-5>
- 986 RStudio Team, 2021. RStudio: Integrated Development Environment for R.
- 987 Sapoval, N., Liu, Y., Lou, E.G., Hopkins, L., Ensor, K.B., Schneider, R., Stadler, L.B., Treangen, T.J., 2023.  
988 Enabling accurate and early detection of recently emerged SARS-CoV-2 variants of concern in  
989 wastewater. *Nat. Commun.* 14, 2834. <https://doi.org/10.1038/s41467-023-38184-3>
- 990 Shu, Y., McCauley, J., 2017. GISAID: Global initiative on sharing all influenza data – from vision to  
991 reality. *Eurosurveillance* 22, 30494. <https://doi.org/10.2807/1560-7917.ES.2017.22.13.30494>
- 992 Silva, C.S., Tryndyak, V.P., Camacho, L., Orloff, M.S., Porter, A., Garner, K., Mullis, L., Azevedo, M.,  
993 2022. Temporal dynamics of SARS-CoV-2 genome and detection of variants of concern in  
994 wastewater influent from two metropolitan areas in Arkansas. *Sci. Total Environ.* 849,  
995 157546. <https://doi.org/10.1016/j.scitotenv.2022.157546>
- 996 Smyth, D.S., Trujillo, M., Gregory, D.A., Cheung, K., Gao, A., Graham, M., Guan, Y., Guldenpfennig, C.,  
997 Hoxie, I., Kannoly, S., Kubota, N., Lyddon, T.D., Markman, M., Rushford, C., San, K.M.,  
998 Sompanya, G., Spagnolo, F., Suarez, R., Teixeira, E., Daniels, M., Johnson, M.C., Dennehy, J.J.,  
999 2022. Tracking cryptic SARS-CoV-2 lineages detected in NYC wastewater. *Nat. Commun.* 13,  
1000 635. <https://doi.org/10.1038/s41467-022-28246-3>
- 1001 Swift, C.L., Isanovic, M., Velez, K.E.C., Sellers, S.C., Norman, R.S., 2022. Wastewater surveillance of  
1002 SARS-CoV-2 mutational profiles at a university and its surrounding community reveals a 20G  
1003 outbreak on campus. *PLOS ONE* 17, e0266407.  
1004 <https://doi.org/10.1371/journal.pone.0266407>
- 1005 Tamáš, M., Potocarova, A., Konecna, B., Klucar, L., Mackulak, T., 2022. Wastewater Sequencing-An  
1006 Innovative Method for Variant Monitoring of SARS-CoV-2 in Populations. *Int. J. Environ. Res.*  
1007 *Public. Health* 19, 9749. <https://doi.org/10.3390/ijerph19159749>
- 1008 Tao, K., Tzou, P.L., Nouhin, J., Gupta, R.K., de Oliveira, T., Pond, S.L.K., Fera, D., Shafer, R.W., 2021.  
1009 The biological and clinical significance of emerging SARS-CoV-2 variants. *Nat. Rev. Genet.* 22,  
1010 757–773. <https://doi.org/10.1038/s41576-021-00408-x>
- 1011 The UniProt Consortium, 2023. UniProt: the Universal Protein Knowledgebase in 2023. *Nucleic Acids*  
1012 *Res.* 51, D523–D531. <https://doi.org/10.1093/nar/gkac1052>
- 1013 Valieris, R., Drummond, R.D., Defelicibus, A., Dias-Neto, E., Rosales, R.A., Tojal da Silva, I., 2022. A  
1014 mixture model for determining SARS-Cov-2 variant composition in pooled samples.  
1015 *Bioinformatics* 38, 1809–1815. <https://doi.org/10.1093/bioinformatics/btac047>
- 1016 Van Rossum, G., Drake, F.L., 2009. Python 3 Reference Manual. CreateSpace, Scotts Valley, CA.

- 1017 WHO, 2023. . Track. SARS-CoV-2 Var. URL [https://www.who.int/en/activities/tracking-SARS-CoV-2-](https://www.who.int/en/activities/tracking-SARS-CoV-2-variants/)  
1018 [variants/](https://www.who.int/en/activities/tracking-SARS-CoV-2-variants/) (accessed 6.20.23).
- 1019 Wickham, H., 2016. ggplot2: Elegant Graphics for Data Analysis., Use R! Springer International  
1020 Publishing. <https://doi.org/10.1007/978-3-319-24277-4>
- 1021 Wickham, H., François, R., Henry, L., Müller, K., Vaughan, D., Software, P., PBC, 2023a. dplyr: A  
1022 Grammar of Data Manipulation.
- 1023 Wickham, H., Hester, J., François, R., Bryan, J., Bearrows, S., Posit, PBC, library), [https://github](https://github.com/mandreyel/mio)  
1024 [com/mandreyel/](https://github.com/mandreyel/mio) (mio, implementation), J.J. (grisu3, implementation), M.J. (grisu3, 2023b.  
1025 readr: Read Rectangular Text Data.
- 1026 Wickham, H., Pedersen, T.L., Software, P., PBC, 2023c. gtable: Arrange “Grobs” in Tables.
- 1027 Wilke, C.O., 2020. cowplot: Streamlined Plot Theme and Plot Annotations for “ggplot2.”
- 1028 Wu, Y., Guo, C., Tang, L., Hong, Z., Zhou, J., Dong, X., Yin, H., Xiao, Q., Tang, Y., Qu, X., Kuang, L., Fang,  
1029 X., Mishra, N., Lu, J., Shan, H., Jiang, G., Huang, X., 2020. Prolonged presence of SARS-CoV-2  
1030 viral RNA in faecal samples. *Lancet Gastroenterol. Hepatol.* 5, 434–435.  
1031 [https://doi.org/10.1016/S2468-1253\(20\)30083-2](https://doi.org/10.1016/S2468-1253(20)30083-2)  
1032